AD-A168 816 GAS PHASE REACTIONS OF DIMETHOXY PHOSPHORYL ANION (CH3O)2PO(-)(U) ARMY MILITARY PERSONNEL CENTER ALEXANDRIA VA K D DEWITT 13 MAY 86 1/1

UNCLASSIFIED F/G 7/4 NL

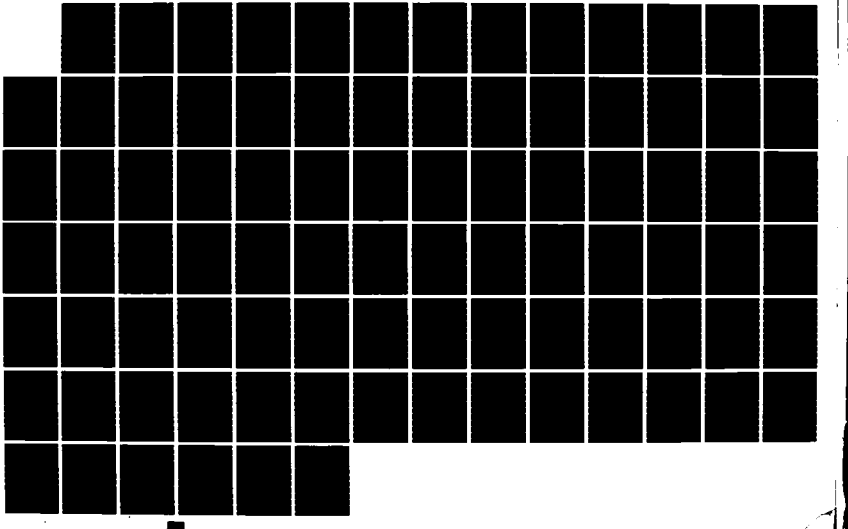

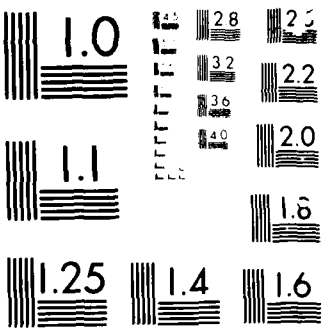
1.0
1.1
1.25
1.4
1.6
2.8
3.2
3.6
4.0
2.2
2.0
1.8

SECURITY CLASSIFICATION OF THIS PAGE (When Data Entered)

REPORT DOCUMENTATION PAGE	READ INSTRUCTIONS BEFORE COMPLETING FORM
1. REPORT NUMBER / 2. GOVT ACCESSION NO.	3. RECIPIENT'S CATALOG NUMBER
4. TITLE (and Subtitle) Gas Phase Reactions of Dimethoxy Phosphoryl Anion $(CH_3O)_2PO^-$	5. TYPE OF REPORT & PERIOD COVERED Final Report 13 May 86
	6. PERFORMING ORG. REPORT NUMBER
7. AUTHOR(s) CPT Krisma D. DeWitt	8. CONTRACT OR GRANT NUMBER(s)
9. PERFORMING ORGANIZATION NAME AND ADDRESS Student, HQDA, MILPERCEN (DAPC-OPA-E) 200 Stovall Street, Alexandria, Virginia 22332	10. PROGRAM ELEMENT, PROJECT, TASK AREA & WORK UNIT NUMBERS
11. CONTROLLING OFFICE NAME AND ADDRESS HDDQ, MILPERCEN (DAPC-OPA-E) 200 Stovall Street, Alexandria, Virginia 22332	12. REPORT DATE 13 May 86
	13. NUMBER OF PAGES 85
14. MONITORING AGENCY NAME & ADDRESS(if different from Controlling Office)	15. SECURITY CLASS. (of this report) Unclassified
	15a. DECLASSIFICATION DOWNGRADING SCHEDULE

16. DISTRIBUTION STATEMENT (of this Report)

Approved for public release; distribution unlimited.

17. DISTRIBUTION STATEMENT (of the abstract entered in Block 20, if different from Report)

18. SUPPLEMENTARY NOTES

Master's Thesis
Kansas State University, Manhattan, KS 66506

19. KEY WORDS (Continue on reverse side if necessary and identify by block number)

Dimethoxy phosphoryl anion
Gas phase reactions
Kinetics
Phosphorus compounds
$S_{RN}1$ mechanism

20. ABSTRACT (Continue on reverse side if necessary and identify by block number)

On back

DD FORM 1 JAN 73 1473 EDITION OF 1 NOV 65 IS OBSOLETE

Block 20 (cont)

ABSTRACT

Dimethoxy phosphoryl anion [$(CH_3O)_2PO^-$] was generated in the gas phase by ion-molecule reaction using phenyl nitrene anion radical [PhN^-] to abstract a proton. Phenyl nitrene was generated by dissociative electron attachment with phenyl azide [PhN_3] in a flowing afterglow apparatus. Using bracketing studies of ion-molecule reactions of $(CH_3O)_2PO^-$ with potential proton-donor molecules of known acidity, PA[$(CH_3O)_2PO^-$] was determined to be 358 $\pm$ 2 kcal/mol and ΔH_f^o[$(CH_3O)_2PO^-$] was calculated to be -207.3 $\pm$ 2 kcal/mol. The electron affinity, EA[$(CH_3O)_2P(=O)^{\bullet}$], was also investigated using the bracketing technique and was found to be 2.2 $\pm$ 0.1 eV.

Reactions of $(CH_3O)_2PO^-$ with methyl halides indicate that the dimethoxy phosphoryl anion is an ambident species of low intrinsic nucleophilicity. $(CH_3O)_2PO^-$ reacts through electron transfer process with numerous halogenated alkanes. The dimethoxy phosphoryl anion has been found to form very stable hydrogen bonded complexes with various neutral organic and inorganic complexes.

The reactions of the hydrogen bonded adduct of dimethyl phosphite and dimethoxy phosphoryl anion, $(CH_3O)_2PO^-/H(O=)P(OCH_3)_2$, was also investigated with the same neutral substrates. Its reactions are similiar to those of the dimethoxy phosphoryl anion.

Gas Phase Reactions of Dimethoxy Phosphoryl Anion $(CH_3O)_3PO^-$

CPT Krisma D. DeWitt
HQDA, MILPERCEN (DAPC-OPA-E)
200 Stovall Street
Alexandria, VA 22332

Final Report, 13 May 1986

A thesis submitted to Kansas State University, Manhattan, KS 66506 in partial fulfillment of the requirements for the degree of Masters of Science.

GAS PHASE REACTIONS OF DIMETHOXY PHOSPHORYL ANION

$((CH_3O)_2PO^-)$

by

KRISMA DEYLENE DEWITT

B. S., South Dakota State University, 1978

AN ABSTRACT OF A MASTER'S THESIS

submitted in partial fulfillment of the

requirements for the degree

MASTER OF SCIENCE

Department of Chemistry

KANSAS STATE UNIVERSITY

Manhattan, Kansas

1986

ABSTRACT

Dimethoxy phosphoryl anion [$(CH_3O)_2PO^-$] was generated in the gas phase by ion-molecule reaction using phenyl nitrene anion radical [$PhN^{\cdot-}$] to abstract a proton. Phenyl nitrene was generated by dissociative electron attachment with phenyl azide [PhN_3] in a flowing afterglow apparatus. Using bracketing studies of ion-molecule reactions of $(CH_3O)_2PO^-$ with potential proton-donor molecules of known acidity, $PA[(CH_3O)_2PO^-]$ was determined to be 358 $\pm$ 2 kcal/mol and $\Delta H_f^\circ[(CH_3O)_2PO^-]$ was calculated to be -207.3 $\pm$ 2 kcal/mol. The electron affinity, $EA[(CH_3O)_2P(=O)^{\cdot}]$, was also investigated using the bracketing technique and was found to be 2.2 $\pm$ 0.1 eV.

Reactions of $(CH_3O)_2PO^-$ with methyl halides indicate that the dimethoxy phosphoryl anion is an ambident species of low intrinsic nucleophilicity. $(CH_3O)_2PO^-$ reacts through electron transfer process with numerous halogenated alkanes. The dimethoxy phosphoryl anion has been found to form very stable hydrogen bonded complexes with various neutral organic and inorganic complexes.

The reactions of the hydrogen bonded adduct of dimethyl phosphite and dimethoxy phosphoryl anion, $(CH_3O)_2PO^-/H(O=)P(OCH_3)_2$, was also investigated with the same neutral substrates. Its reactions are similiar to those of the dimethoxy phosphoryl anion.

GAS PHASE REACTIONS OF DIMETHOXY PHOSPHORYL ANION

$((CH_3O)_2PO^-)$

by

KRISMA DEYLENE DEWITT

B. S., South Dakota State University, 1978

A MASTER'S THESIS

submitted in partial fulfillment of the

requirements for the degree

MASTER OF SCIENCE

Department of Chemistry

KANSAS STATE UNIVERSITY

Manhattan, Kansas

1986

Approved by:

Major Professor

TABLE OF CONTENTS

List of Tables

List of Figures

I. INTRODUCTION

Studies of the chemistry of organophosphorus compounds are important in determining their potential use as reagents in synthetic chemistry, their possible industrial applications, and in understanding many biological processes. Dialkyl phosphites are neutral compounds used in the synthesis of insecticides, pesticides, plastics and pharmaceuticals. They are also used as stabilisers for plastics, oil additives, flame retardants, and corrosion inhibitors.[1]

One class of organophosphorus compounds also act as poisons and have been used in the development of chemical and biological weapons. Phosphate esters of the general form in 1, display these

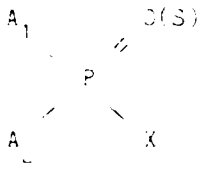

1

characteristics. A_1 and A_2 are groups that are difficult to displace (i.e. alkoxy, dialkylamino, or alkyl groups) and X is a fairly good leaving group (i.e. F^- or $p\text{-}NO_2\text{-}C_6H_4O^-$).[2] These organophosphorus compounds act as inhibitors of enzymes that are involved in nerve functions. Such toxic compounds are inherently good phosphorylating agents. Slight variations in structure of these compounds can cause a drastic affect in the efficiency of the poison. This is probably due to fact that the size, shape, and polarizability of the substrate affect the interation of tne enzyme with the organophosphorus compound. It is believed that these compounds initially form a complex, e.g. 2, with the

enzyme being attacked and then combine chemically to form a stable phosphorylated enzyme (eq 1 and 2). The resulting phosphorylated enzyme is no longer catalytically active.[3]

$$\text{Enzyme} + (A_1)(A_2)(X)P{=}O(\text{or S}) \rightleftharpoons (\text{Enzyme})(A_1)(A_2)(X)P{=}O(\text{or S}) \quad (1)$$

$$\underline{2} \longrightarrow (\text{Enzyme})(A_1)(A_2)P{=}O(\text{or S}) + HX \quad (2)$$

The intrinsic properties of such organophosphorus compounds is of interest in understanding how and why they react and in the further development of applications. Solution phase studies are extensive and have provided a large set of characteristics of compounds of this type. There has, however, been little published literature on gas-phase studies of the intrinsic properites of organophosphorus compounds.

Previous published data concerning the study of organophosphorus compounds in the gas-phase has been limited to ion cyclotron resonance spectroscopy studies of trimethyl phosphite, trimethyl phosphate, triethyl phosphate, and trimethyl phosphorothionate,[4] the gas phase chemistry of trimethyl phosphite,[5] the gas-phase proton affinities of cyclic phosphites,[6] the reactions of phosphine[7,8] and methyl phosphine,[9] negative ion formation by phosphorus trifluoride,[10] nucleophilic reactions of anions with PF_3 and OPF_3,[11] and the gas-phase hydrolysis of phosphorus esters.[12]

Solution-phase reactions of alkyl phosphite esters are fairly well characterized with many references available summarizing these properties. Ionic reactions of these esters fall into three categories:[2]

1) reactions of a trivalent phosphorus center as a nucleophile by virtue of the non-bonding 3s electrons,
2) nucleophilic displacement at phosphorus, and
3) reactions that do not involve the phosphorus center directly.

Dialkyl phosphite esters, $(RO)_2POH$, show very little nucleophilic character whereas the trialkyl phosphites, $(RO)_3P$, do function as nucleophiles as illustrated in the Arbuzov reaction (eq 3).[2] The dialkyl

$$(C_2H_5O)_3P: + CH_3I \longrightarrow (C_2H_5O)_2P(=O)CH_3 + C_2H_5I \qquad (3)$$

phosphite are also only weakly acidic; the pK_a of $(C_2H_5O)_2P(=O)H$ has been estimated to be approximately 15.[2] The low nucleophility of the dialkyl phosphites can be attributed to the fact that phosphite compounds of the general structure $(RO)_2POH$ can exist in two tautomeric structures, the phosphite form 3 and the phosphonate form 4.[2] The di-

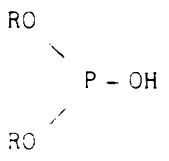

3

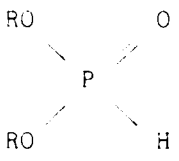

4

alkyl phosphonate structure 4 does not have a lone pair of electrons on phosphorus to contribute to nucleophilic character. The phosphonate form is believed to be the reactive intermediate in several reactions.[3]

There has long been a controversy in solution chemistry concerning the structure of these compounds. It has, however, been established that these two structures are in equilibrium. Studies of the tautomerizm of dimethyl phosphonate were the topic of a report by Pietro and Henre.[13] Experiments were conducted to determine the difference in

the heats of formation of the two isomers; the phosphonate isomer was 6.5 kcal/mole more stable than the phosphite isomer in the gas phase. This predominance of the phosphonate structure is presumed to arise from the stability of a very strong P=O bond.[13] In general, the relative stabilities of the neutral compound has been used in assigning relative stabilities to the corresponding positive ions. It has, therefore, been assumed that positively charged ions containing a P(=O)H group are more stable than the tautomer containing the POH group.[14] This correlation, however, may not be valid due to that fact that the relative stabilities of gas-phase ions are not necessarily in direct agreement with their corresponding gas-phase neutrals.[14] One of the driving forces for gas-phase reactions of ionized organophosphorus esters appears to be the formation of the P-OH structures.

Most of the work done in determining relative stability of ions in the gas-phase has been done with positive ions.[15] Evidence has indicated that keto and enol cations are distinct stable species in the gas phase. The enol ions transfer their hydroxylic proton to a suitable species in an ICR cell whereas the keto ions do not react by proton transfer.[16]

An extensive thermochemical study of $C_nH_{2n}O^{+\cdot}$ and $C_nH_{2n}O_2^{+\cdot}$ was conducted by Holmes and Lossing.[17] They determined the relative stabilities of these ions compared to their ionized isomeric carbonyl compounds. It was found that the enolic ions investigated were all more stable than their keto tautomers by 14 to 31 kcal/mol. This is a marked contrast to the neutral tautomers where the keto forms are usually the more stable form.[17]

Recent work[16] has shown that dimethyl methylphosphonate ion undergoes slow isomerization from the keto to the enol isomer following ionization to the positive ion (eq 4). Through the use of energy re-

$$(CH_3O)_2P(=O)CH_3^{+\cdot} \longrightarrow (CH_3O)_3P^{+\cdot} \qquad (4)$$

solved mass spectrometry, a study concluded that the phosphite ion radical tautomer is 1.2 eV (27 kcal/mol) more stable than the phosphonate ion radical tautomer. In constrast, in the neutral molecules the phosphonate tautomer is the more stable form.[14] Thus, tnere is a very strong tendency for organophosphorus ester cation radical to form the POH group in the gas phase. This also suggests that the proton transfer to the ionized organophosphorus ester ion in the gas phase most likely occurs at the oxygen rather than the phosphorus atom.

Reaction of halogens with neutral phosphorus compounds containing at least one alkoxy group may result in the dealkylation of the phosphonium compound (eq 5). The second stage of this reaction is similiar to tne second step of the Arbusov reaction. In the condensed phase, di-

$$R'_2P(=O)R + X_2 \longrightarrow R'_2\overset{+}{P}\!\!<\!\!\begin{matrix} X \\ O\!-\!R \end{matrix}\; X^- \longrightarrow R'_2P(=O)X + RX \qquad (5)$$

alkyl phosphites can be easily oxidized to phosphorochloridates (eq 6) with the other product being a hydrogen halide as the byproduct. The reactive species is believed to be the phosphite tautomer and the rate

$$(RO)_2P(=O)H + X_2 \longrightarrow (RO)_2P(=O)X + HX \qquad (6)$$

rate controlling step is the isomerization of the phosphorus compound from phosphonate to the phosphite isomer.[2]

Dialkyl phosphite anions (hereafter called dialkoxy phosphoryl anions) react with alkyl halides in solution by an S_N2-type mechanism

forming dialkyl alkyl phosphonates and halide ion (eq 7).[2] The reaction is assumed to be bimolecular.

$$(RO)_2P(=O)^- + R'X \longrightarrow (RO)_2P(=O)R' + X^- \quad (7)$$

Dialkyl phosphites add readily to carbonyl groups (eq 8) of simple aldehydes and ketones yeilding adducts; the product are 1-hydroxyalkyl-1-phosphonate esters.[2] The reaction is catalyzed by strong base and the

$$(RO)_2P(=O)H + R'CHO \longrightarrow (RO)_2P(=O)CHOHR' \quad (8)$$

reactive species is presumed to be the dialkoxy phosphoryl anion. This addition of the dialkyl phosphite to the carbonyl group is reversible, but the equilibrium favors addition under normal conditions.[2]

Dialkoxy phosphoryl anions are oxidized by carbon tetrachloride (eq 9). A free radical mechanism has been ruled out and it is believed that initial attack on the C-Cl bond occurs.[2]

$$(RO)_2P(=O)^- + CCl_4 \longrightarrow (RO)_2P(=O)Cl + CCl_3^- \quad (9)$$

Solution-phase studies[17] of the ionization of the P-H bond in diethyl phosphonate, $(C_2H_5O)_2P(=O)H$, indicate that proton transfer from phosphorus are below the diffusion-controlled limit; in the gas phase phosphites equilibrate with protonated species at fast rates by ICR standards.[6] In a study by Lewis and Spears,[18] reaction kinetics for the reaction of dialkyl phosphonate with I_2 were investigated. The report concluded that the oxidation process for P-H compounds is anolagous to the ionization of a C-H α to a carbonyl group or a nitro group where the proton transfer in solution phase is also slower than the diffusion-controlled rate.

Metaphosphates, generalized in structure 5, have never been isolated, but their existance as transient intermediates has been

deduced from kinetic and stereochemical data.[3] The metaphosphite anion (PO_3^-) has been proposed as an intermediate in phosphorylation reactions, the hydrolysis of mono esters of phosphoric acid, and hydrolysis of various esters of pyrophosphoric acid.[19]

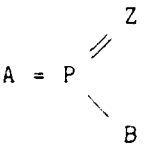

5

Westheimer, et al.,[20] directed studies towards identifying monomeric methyl metaphosphate, CH_3OPO_2, generated by Conant-Swan fragmentation of eyrtho- and threo-1-phenyl-1,2-dibromopropyl phosphonates in the presence of 2,2,6,6-tetramethylpiperidine. This group was successful in trapping the methyl metaphosphate reactive intermediate and elucidating some of its chemistry. The same group[21] also was successful in investigating the monomeric metaphosphate anion, PO_3^-, which was generated rapidly at room temperature by the Conant-Swan fragmentation shown in eq 10. PO_3^- reacts at carbonyl groups of acetophenone to form

$$C_6H_5\text{-}CBr\text{-}CHBr\text{-}CH_3 \xrightarrow{\text{base}} C_6H_5CBr{=}CHCH_3 + [PO_3^-] + Br^- + 2BH^+ \quad (10)$$
$$PO_3H_2$$

the enol phosphate. In the presence of aniline and acetophenone, the product is a Schiff base. PO_3^- reacts with ethyl acetate and aniline to form ethyl N-phenylacedtimidate.[21] This study, however, did not settle the question of whetner PO_3^- is free or is solvated in solution. It is a powerful phosphorylating agent.[21]

Ramirez and Merecek[22,23] conducted studies on phosphoryl transfer from 2,4-dinitrophenyl dinydrogen phosphate ($ArPH_2$) in aprotic and

protic solvents. They concluded the monomeric metaphosphate anion was an intermediate in the process involving the dianion $(ArP)^{2-}$ but not in the monoanion $(ArPH)^{-}$. Further research[24] was conducted concerning the reactions of the monomeric metaphosphate anion generated from different sources. The study was conducted using 0.2M acetonitrile solutions of 2,4-dinitro dihydrogen phosphate and erythro-1-phenyl-1,2-dibromopropyl phosphinic acid containing 2 molar equivalents of diisopropylethylamine. ^{31}P NMR spectroscopy was used to follow these reactions. The 2,4-dinitrophenyl phosphate (6), and erythro-1-phenyl-1,2-dibromopropyl phosphonate (7), formed dianions in solution and generate PO_3^- at

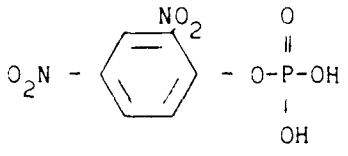

6

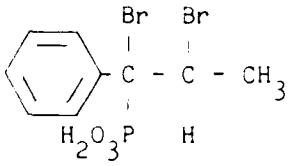

7

different rates. Fragmentation occurs much faster in the phosphonate dianion than in the phosphate dianion. A consequence of the difference in rates of fragmentation is that the phosphate-derived metaphosphate produces cyclic trimetaphosphate, while the phosphonate-dervied species produces acyclic linear and branched polymetaphosphates.[23] Recent work[25] has continued to explore monomeric metaphosphate anions in negative-ion chemical-ionization mass spectra of phosphorus triesters. Clapp and Westheimer[19] were able to produce monomeric metaphosphate in the gas phase by pryolysis of methyl 2-butenylphostonate and trapping with N-metnylaniline. Recent gas-phase studies[25] using negative-ion-chemical-ionization (NICI) techniques to analyse phosphotriesters reports a product at m/z 79 which was attribute to PO_3^-.

The mechanism of hydrolysis of phosphate monoesters continues to be the interest area of numerous studies. Recent work[26] has emphasised that these reactions cannot generate a completely free metaphosphate ion intermediate. It appears that though the metaphosphate is an intermediate in these types of reactions, it does not exist as a free species in solution as it does in the gas phase. PO_3^-, which is proposed as a reactive intermediate in solution, is thermodynamically stable and undergoes no chemical reactions in the gas phase.[27] Cluster ion formation with PO_3^- and the polar molecules HCl, HI, and CH_3CN was, however, observed. Such clusterings are third order reactions involving collisional stabilization by the buffer gas. The rates of cluster ion formation of PO_3^- with HCl, HI, and CH_3CN depends on the ΔH^o_{acid} of the proton donor which correlates to the binding energy of the clusters.[28]

Hydrogen bonding of protic substrates to negative ions in the gas phase has been an extensively investigated area.[28] Relative hydrogen bonding energies have been determined using measurements of ionic equilibria for reactions $(BHR)^- = B^- + HR$. The results suggest that the hydrogen-bond energies increase with the increasing bacisity of B^- and decreasing acidity of HR.

One utility of dialkoxy phosphoryl anions in organic chemistry has been in their use to effect overall S_N2-type displacements of aryl halides. These reactions have been shown to occur by the $S_{RN}1$ mechanism[29] first described by Kornblum[30] and Russell.[31] This mechanism involves substitution at a saturated or unsaturated carbon atom in a molecule, but proceeds via a chain reaction mechanism involving radical anions and free radicals as intermediates. This type of reaction

belongs to the general class of electron transfer induced reactions.[32] There are a number of substituent groups which do not act as leaving groups in S_N2 displacements that are readily displaced at room temperature via a radical anion free radical pathway, for example the nitro, azide, sufone, and ether groups.[30]

Aromatic nucleophilic substitution proceeding by the $S_{RN}1$ mechanism is a well documented area.[29,33] Recent studies in this area have been examined electrochemically to determine absolute reactivities of benzene derivatives[32] and aryl radical reactivity in $S_{RN}1$ aromatic nucleophilic substitution reactions.[34] The initiation and propagation steps in the $S_{RN}1$ reaction mechanism are given in eqs 11-13.[30] The e^- in eq 10 is an electron source and eq 12-14 are the propagation steps. The initial reduction process (eq 11) can be initiated photochemically, electrochemically, by alkali metals in liquid ammonia, or by one-electron reducing agents.[32,34] In this initiation step (eq 11), the aryl halide captures an electron. This radical anion then dissociates to form an aryl radical plus halide ion (eq 12). The aryl radical then reacts with the nucleophilic anion to form a new ion radical (eq 13). This new ion radical reacts with the neutral aryl substrate by electron transfer to give the substitution product and regenerates the anion radical which propagates the chain reaction (eq 14).[33]

$$ArX + e^- \rightleftharpoons ArX^{\cdot-} \qquad (11)$$

$$ArX^{\cdot-} \overset{k_1}{\rightleftharpoons} Ar^{\cdot} + X^- \qquad (12)$$

$$Ar^{\cdot} + Nu^- \overset{k_2}{\rightleftharpoons} ArNu^{\cdot-} \qquad (13)$$

$$ArNu^{\cdot-} + ArX \rightleftharpoons ArNu + ArX^{\cdot-} \qquad (14)$$

Dialkoxy phosphoryl anions, in particular $(C_2H_5O)_2PO^-$, have been used as nucleophiles to investigate the $S_{RN}1$ mechanism.[33] $(C_2H_5O)_2PO^-K^+$ reacts with aryl iodides in liquid ammonia to form the diethyl ester of the aryl phosphonic acid shown in eq 15.[35,38] There is no observed reaction in the dark indicating that the reaction is photochemical in

$$ArI + (C_2H_5O)_2PO^- \xrightarrow{h\nu} ArP(O)(OC_2H_5)_2 + I^- \qquad (15)$$

nature. This reaction has been studied with m-halo-iodobenzenes where m-halo = I, Br, Cl, F. The m-fluoro- and m-chloroiodobenzene gave mainly monosubstituted products whereas the m-diiodobenzene and m-bromoiodobenzene compounds give disubstituted products.[37,38] Similiar experiments were performed using p-haloiodobenzenes with analogous results.[38] The results of the experiments were explained with the $S_{RN}1$ mechanism with two competative reactions occuring. One of the competing reactions is the electron transfer from a monosubstituted anion radical to the neutral substrate which yields the monosubstituted product. The other is the C-X bond cleavage of the same monosubstituted anion radical to give halide anion and the substituted aryl radical. The substituted aryl radical further reacts to give the disubstituted product. The difference in whether monosubstituted or disubstituted products are produced seems to depend on the halogen involved.[38]

$S_{RN}1$ reactions have also been noted in purely aliphatic systems. A typical system displaying this type of reaction is the displacement of a nitro group from α-nitro esters, α-nitro ketones, α-nitro nitriles, and α,α-dinitro compounds.[24] The mechanistic pathway in eq 16-19 was proposed for the α-nitro ester systems.[30]

$$(CH_3)_2\underset{NO_2}{\overset{|}{C}}\text{-COOR} + (CH_3)_2\bar{C}\text{-}NO_2 \longrightarrow (CH_3)_2\underset{NO_2^{\cdot}}{\overset{|}{C}}\text{-COOR} + (CH_3)_2\dot{C}\text{-}NO_2 \qquad (16)$$

$$(CH_3)_2\underset{NO_2^{\cdot}}{\overset{|}{C}}\text{-COOR} \longrightarrow (CH_3)_2\dot{C}\text{-COOR} + NO_2^- \qquad (17)$$

$$(CH_3)_2\dot{C}\text{-COOR} + (CH_3)_2\bar{C}\text{-}NO_2 \longrightarrow \begin{matrix}(CH_3)_2\text{-}\overset{|}{C}\text{-COOR} \\ (CH_3)_2\text{-}C\text{-}NO_2^{\cdot}\end{matrix} \qquad (18)$$

$$\begin{matrix}(CH_3)_2\text{-}\overset{|}{C}\text{-COOR} \\ (CH_3)_2\text{-}C\text{-}NO_2^{\cdot}\end{matrix} + (CH_3)_2\underset{NO_2}{\overset{|}{C}}\text{-COOR} \longrightarrow \begin{matrix}(CH_3)_2\underset{(CH_3)_2C\text{-}NO_2}{\overset{|}{C}}\text{-COOR} \\ \end{matrix} + (CH_3)_2\underset{NO_2^{\cdot}}{\overset{|}{C}}\text{-COOR} \qquad (19)$$

The reactions of trimethyl phosphite [$(CH_3O)_3P$] were studied in the gas phase with various anionic nucleophiles, and the products, branching ratios, and reaction rate constants were reported.[5] The reactions reported by this work were divided into two types. Anions with acidic hydrogens, e.g. CH_3NH^-, reacted with $(CH_3O)_3P$ by addition and loss of methanol (eq 20). However, anions without acidic hydrogens, e.g.

$$CH_3NH^- + (CH_3O)_3P \longrightarrow (CH_3O)_2PNCH_3^- + CH_3OH \qquad (20)$$

CH_3O^-, reacted with trimethyl phosphite to produce dimethoxy phosphoryl anion [$(CH_3O)_2PO^-$] and the adduct, $(CH_3O)_4P^-$. Using labeling experiments, results of this investigation were interpreted as an initial attack on the phosphorus center resulting in the displacement of methoxide anion. Methanol is formed by the abstraction of a proton if available. If the reaction products remain in an ion-dipole association

complex for a long enough time, further reactions are possible such as exothermic proton transfer or formation of a stable dimethoxy phosphoryl anion. The product branching ratios are dependent on the thermodynamics of tne ion-dipole complex equilibrium. In this study, the gas phase acidity of $(CH_3O)_2PO^-$ was determined using the bracketing technique and found to be 357 $\pm$ 3 kcal/mol.

The gas-phase hydrolysis of phosphorus esters was studied by Asubiojo and Brauman.[12] In solution, there is a remarkable difference in rates of hydrolysis of cyclic phosphorus esters. This has been attributed to effects of strain and energetics on trigonal-bipyramidal intermediates in these reactions. The gas-phase rates of reaction of tne cyclic phosphorus esters and trimethyl phosphate with OH^- were measured using trapped ion, pulsed ICR techniques. Results showed that tne strain effects persist in the gas-phase and are not due to solvation effects.

Gas-phase positive ion-molecule studies have been conducted on reactions of trimethyl phosphate, triethyl phosphate and trimethyl phosphorothionate. These studies were conducted using ion cyclotron resonance spectroscopy.[4] The reactions in this study were catagerized as (a) reactions in which a tetracoordinated phosphoniom ion was formed, and (b) clustering reactions. An example of a type (a) is shown in eq 21.

$$OP(OCH_3)_2^+ + P(OCH_3)_3 \longrightarrow P(OCH_3)_4^+ + OPOCH_3 \qquad (21)$$

Clusters of proton-bound dimers (eq 22) were noted along with clusters

$$HOP(OC_2H_5)_3^+ + OP(OC_2H_5)_3 \longrightarrow H(OP(OC_2H_5)_3)_2^+ \quad (22)$$

of the general structure $P_2X_a(OCH_3)_b$ where X = O and S, a = 0-2, and b = 3, 5 or 6. This clustering was explained as the result of donation of lone pair electrons from the neutral to the phosphorus atom of the ion, for example $(CH_3O)_3P^+$-$OP(=O)(OCH_3)_2$.

Other gas phase studies of phorphorus compounds that have been published include ion cyclotron resonance spectroscopy studies of nucleophilic reactions of anions with PF_3 and OPF_3,[11] gas phase proton affinities of cyclic phosphites,[6] and negative ion formation studies of PF_3 as a result of electron bombardment.[10]

II. OBJECTIVES

The objectives of this investigation were (1) to generate dimethoxy phosphoryl anion [$(CH_3O)_2PO^-$] in the gas phase, (2) to determine the proton affinity (PA) and heat of formation (ΔH_f^o) of $(CH_3O)_2PO^-$, and electron affinity (EA) of $(CH_3O)_2\dot{P}O$, (3) to study the reactivity of $(CH_3O)_2PO^-$ with a variety of organic and inorganic molecules, and (4) to model and investigate electron transfer reactions with $(CH_3O)_2PO^-$ in an attempt to model this step in the $S_{RN}1$ mechanism.

III. EXPERIMENTAL METHOD

The flowing afterglow (FA) apparatus was chosen to study the gas phase reactions of $(CH_3O)_2PO^-$, m/z 109, and the hydrogen bonded adduct, $(CH_3O)_2PO^-/H(O=)P(OCH_3)_2$, m/z 219, at 298K. The design, theory, and operation of the FA apparatus have been reviewed.[39] The specific apparatus of this laboratory has been described [40,41] and is shown in Figure 1.

The FA consists of three regions: (i) the ion production region including the electron gun and inlets 1 - 5, (ii) the ion-molecule reaction region, and (iii) the ion detection region. The main flow tube is a 1.5 m long, 7.15 cm diameter stainless steel pipe of a modular design. A 20 cm long, 4 cm diameter glass side arm containing one of two helium inlets, the electron gun, and inlet 1 is located at the upstream end of the flow tube. The flow tube is attached to a stainless steel box approximately 30 cm X 30 cm X 30 cm divided into three compartments separated by two nose cones with a 1 mm orifice in each. The first compartment is attached to a large, fast pumping system which maintains the fast flow velocity and relatively high pressure of the helium buffer gas in the flow tube during the experiment. The second and third compartments are differentially pumped. The third compartment contains the quadrupole mass filter and electron multiplier which continuouly monitor the ion composition present in the flow tube.

In the present experiments, a large flow of helium buffer gas (99.99%) is passed through Davison 4A molecular sieves in traps cooled by liquid nitrogen for purification of the gas. The buffer gas is warmed to room temperature by passing it through a glass coil and then

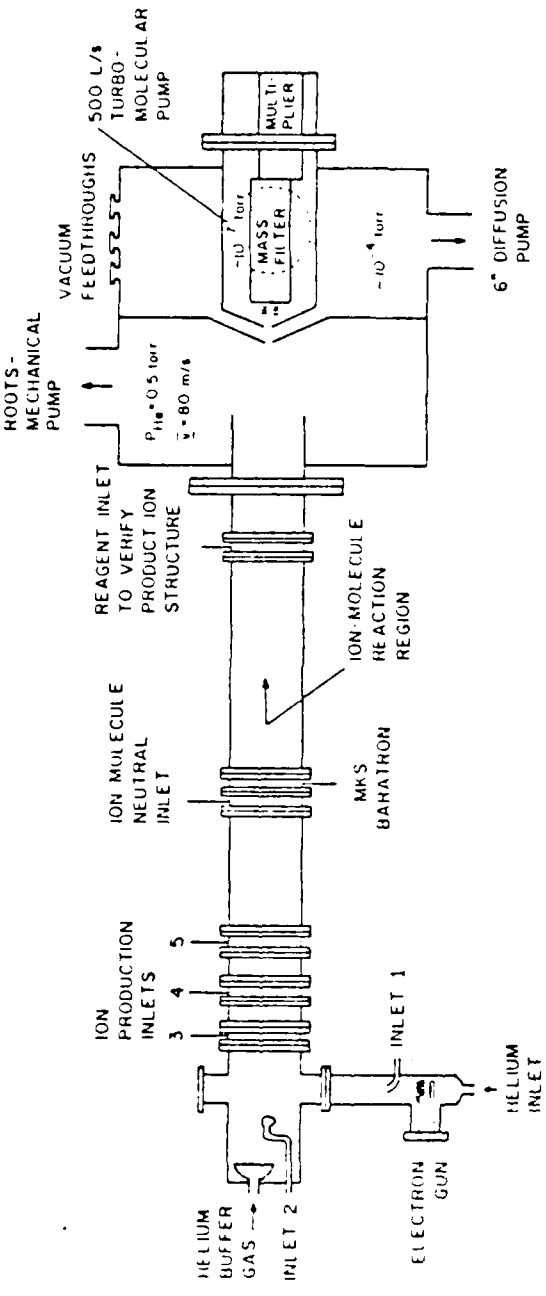

Figure 1. Schematic diagram of the flow tube.

into the two inlets shown in the upstream end of the stainless steel flow tube. The helium mass flow rate (F_{He}) is measured with a Fisher and Porter triflat flowmeter (Model #449-306). The helium flow is then divided with the major part (85-90%) entering the main flow tube and a smaller amount entering the Pyrex glass arm which is measured by a Fisher and Porter triflat flowmeter (Model #449-207). Calibration data for both flow meters was used as supplied by the manufacturer without further testing. The pressure is monitored with a Baritron MKS 0-1000 torr pressure transducer. The pressure of the helium buffer gas in the flow tube was variable from 0.3 to 1.2 torr through the use of a throttling valve and control of the helium flow. The pressure in the flow tube can be varied from P_{He} = 0.3 to 1.2 torr and the flow velocity is variable from $\bar{v}$ = 30 to 80 m sec^{-1}. Standard conditions used in these experiments were P_{He} = 0.5 torr, $\bar{v}$ = 80 m sec^{-1}, and F_{He} = 212 cm^3 sec^{-1}. Reactions were conducted at 0.5 and 1.0 torr to determine if P_{He} effects could be observed for each neutral reacted with $(CH_3O)_2PO^-$. A Stokes Roots blower-mechanical pump system (Model 1722-S) was used to establish and maintain the helium flow parameters.

Electrons are generated using an electron gun consisting of either a rhenium filament or a thorium oxided coated iridium filament located 1 cm upstream of a grounded stainless steel mesh grid. Electrons are emitted from the filiament which is heated with current supplied by a Hewlett Packard (Model #6286A) DC power supply superimposed over a -100V potential (relative to the grounded stainless steel grid) from a Keithly high voltage power supply (Model #245). The emission current at the electron gun was measured by inserting a Micronta VOM (Model #22-207a) in the circuit between the filament and the grid. The emission current

is a measure of the number of charged particles, electrons and ions, formed in the vicinity of the filament and striking the grounded grid. The emission current was typically 200 microamps with 4.5 amp supplied to the filament by the DC power supply.

In the first 70 cm of the flow downstream of the electron gun, ion production and thermalization occur. The negative ions are initially formed vibrationally excited and are cooled to their vibrational ground state by collisions with the helium buffer gas in this region. This region also allows for the establishment of a laminar flow in the flow tube. The remaining distance of the flow tube to the first nose cone is the reaction region where neutral reagents are allowed to react with the ion of interest. SF_6, which has an electron affinity of 1.00 $\pm$ 0.2 eV,[42] is added at the ion-molecule neutral inlet to insure that all electrons were captured prior to the reaction region. This inlet is fitted with a 2 mm i.d. glass loop with holes every 5 mm on the inside of the loop.

The reaction mixture and its ionic components are sampled via the orifices in the two nose cones into the mass filter-electron multiplier compartment operating at 2×10^{-7} torr containing an Extranuclear C-50 quadrapole mass spectrometer with a mass range of 3 to 1200 amu. The nose cones are insulated by Teflon gaskets and can be biased from 0 to $\pm$ 15 V.

With the system operated at P_{He} = 0.5 torr and $\bar{v}$ = 80 m sec^{-1}, the concentration of the helium buffer gas is 1.6×10^{16} atoms cm^{-3}. The concentration of the added neutral reactant is generally from 10^{11} to 10^{14} molecules cm^{-3}, while the ion concentration is estimated at $<10^{8}$ ions cm^{-3}. These conditions constitute psuedo-first-order kinetic

$$k\ (cm^3\ molecule^{-1}s^{-1}) = \frac{d(\log[I^-])}{d[N](molecules\ cm^{-3})} \times \frac{F_{He}(atm\ cm^3\ s^{-1}) \times (2.78 \times 10^3\ torr\ atm^{-1})}{P_{He}(torr) \times r^2(cm^2) \times D(cm)} \quad (23)$$

conditions and the bimolecular rate constants for the ion-molecule reactions are calculated using eq 23. $[I^-]$ is the integrated ion signal intensity from the mass spectrum of $(CH_3O)_2PO^-$ or its hydrogen bonded adduct anion, F_{He} and P_{He} are the flow rate and flow tube pressure of the helium buffer gas, respectively, r is the radius of the flowtube (3.575 cm), and D is the distance from the ion-molecule neutral reagent inlet to the first sampling nose cone (65.96 cm). The constant in eq 23, 2.78×10^3 torr atm^{-1}, contains a correction value of 1.59 for parabolic flow[43] (2.303 x 760 torr atm^{-1} x 1.59).

The flow of the neutral reactant is measured by determining the increase of pressure in a calibrated volume as a function of time. The neutrals are loaded into 5-L bulbs either as pure material (slow reactions) or diluted with purified helium (fast reactions). These measurements provide [N], the concentration of the neutral added to the flow.

The negative ion products are determined using the Extranuclear C-50 quadrupole mass spectrometer. The ions are detected with a combination conversion dynode (CD)/channeltron electron multiplier. This type of detection provides a good signal to noise ratio and high sensitivity. However, this system can lead to mass discrimination errors, with higher mass polyatomic negative ions being better detected than lower mass or atomic negative ions.[44]

During the experiment, the mass spectrum can be observed on the spectrometers oscilliscope. Spectra of the ions in the flow before and after the addition of a neutral are recorded by passing the analog signal through a fast A/D converter (AI13 from Interactive Structures, Bala Cynwyd, PA) to an Apple IIe computer operated with software developed by Interactive Microware (IMI, State College, PA). To minimize noise, eight spectra are recorded, stored, and then averaged for each data point taken. Normally six data points per kinetic experiment are taken changing the amount of the neutral added for each data point. The averaged spectra are baseline corrected, and integrated (with IMI software) to obtain integrals for the starting and product ions as a function of neutral concentration. Rate constants reported in this paper are the average of at least three kinetic experiments with different loadings (concentrations) of the neutral reactant.

$(CH_3O)_2PO^-$, m/z 109, was generated by ion-molecule reaction of dimethyl phosphite [$(CH_3O)_2P(=O)H$] with phenyl nitrene anion radical [$PhN^{\cdot -}$]. The phenyl nitrene anion radical was generated by dissociative electron attachment with phenyl azide [PhN_3]. The phenyl azide was introduced at inlet 1 (Figure 1), and $(CH_3O)_2P(=O)H$ was introduced at inlet 2. Due to the large amount of $(CH_3O)_2P(=O)H$ needed to eliminate the $PhN^{\cdot -}$ signal, the signal of the hydrogen bonded adduct, $(CH_3O)_2PO^-/H(O=)P(OCH_3)_2$, was also observed at m/z 219 (Figure 2). The rates of reaction of this latter cluster negative ion were also measured.

All of the reactions studied displayed psuedo-first-order decay of $(CH_3O)_2PO^-$ and $(CH_3O)_2PO^-/HP(=O)(OCH_3)_2$ when the log of the ion signal

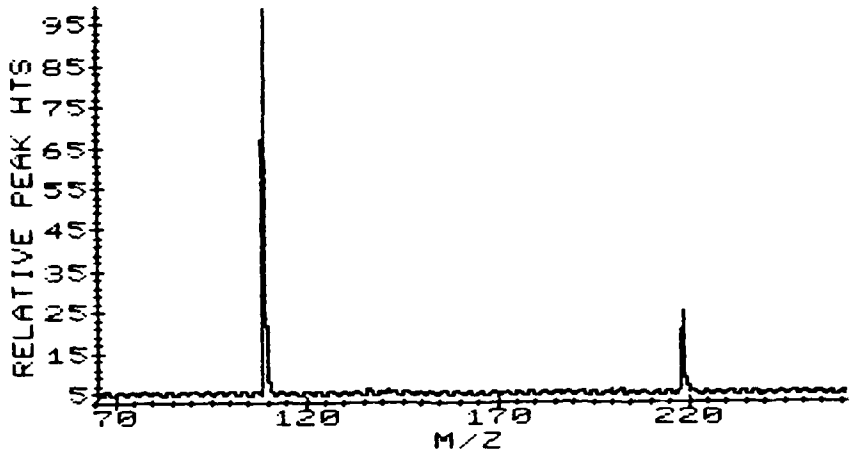

Figure 2. Negative Ion Mass Spectrum Containing $(CH_3O)_2PO^-$ (m/z 109) and $(CH_3O)_2P(=O)H/^-OP(OCH_3)_2$ (m/z 219).

was plotted verses the concentration of the neutral added to the flowtube. A typical plot is shown in Figure 3 for the reaction of $(CH_3O)_2PO^-$ with CCl_4(eq 24). Each point in the figure represents the integrated peak area for each ion at a particular neutral reactant concentration.

$$(CH_3O)_2PO^- + CCl_4 \begin{cases} \longrightarrow CH_3OP(Cl)O_2^- \\ \longrightarrow CCl_3^- \end{cases} \qquad (24)$$

The accuracy of the rate constants (k_{total}) obtained from eq 23 is estimated to be ± 30%, with reproducibility of individual rate constants being within ± 10%. The branching fractions of the product ions are believed to be accurate to ± 15%. The lower accuracy in branching ratios can be attributed to different diffusion rates of ions to flow

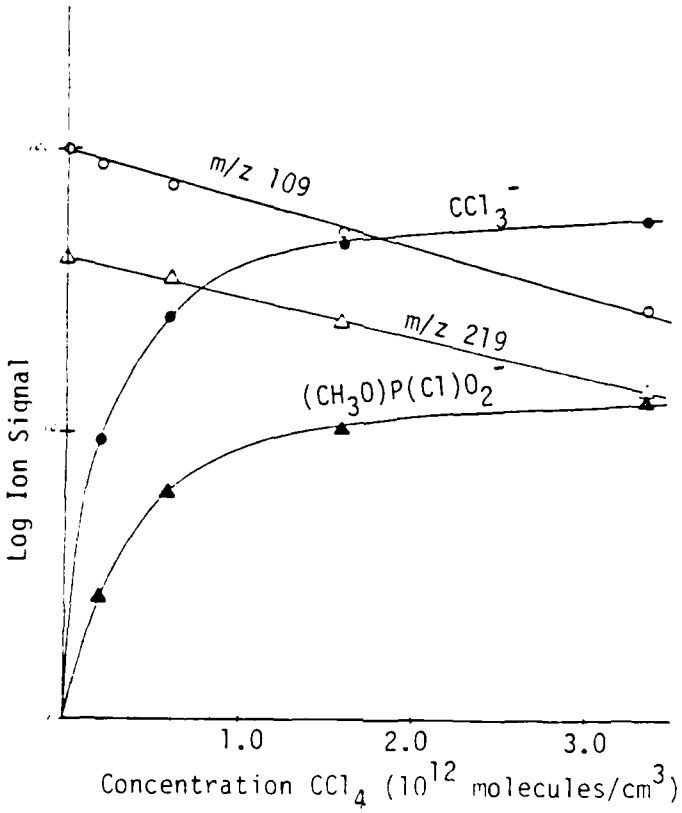

Figure 3. Semilogrithmic plot for the decay of $(CH_3O)_2PO^-$ (m/z 109) and $(CH_3O)_2P(=O)H/^-OP(OCH_3)_2$ (m/z 219) and the formation of CCl_3^- and $(CH_3O)P(Cl)O_2^-$ in the reaction of $(CH_3O)_2PO^-$ with CCl_4.

tube walls, and mass discrimination by the nose cones, the lens assembly, the quadrupole mass filter, and by the electron multiplier.[43,44] Appendix I deals in detail with diffusion in the flow tube and its ramifications on the rate constants and branching fractions as reported in this study.

The formation of $(CH_3O)_2PO/^-H(O=)P(OCH_3)_2$, the hydrogen-bonded cluster ion, will occur throughout the entire length of the flow tube by termolecular coordination of the primary ion $(CH_3O)_2PO^-$ with excess

neutral phosphonate ester present in the gas flow. This means that the "observed" rate constants for loss of the cluster ion from reaction with added neutral molecules will be of no significance since it is made and destroyed in the same region of the flow tube. Since this loss of $(CH_3O)_2PO^-$ forming the hydrogen bonded cluster ion is constant in the experiment, the variable decay of $(CH_3O)_2PO^-$ is caused by the ion-molecule reaction with different concentrations of neutral molecules added to the flow. Thus, the reported rate constants for the reactions of $(CH_3O)_2PO^-$ with neutrals will be accurate within the normal error limits. However, the product channel branching fractions may be in error since the values may be composed of product ions formed from both reactant ions.

The collision limited rate constants for ion-molecule reactions (k_{ADO}) are calculated using the Average Dipole Orientation theory (eq (25).[45,46] The parameters of eq 25 are q = the charge of the ion, μ =

$$k_{ADO} = \frac{2\pi q}{\mu^{1/2}} [\alpha^{1/2} + C\mu_D(2/\pi kT)^{1/2}] \qquad (25)$$

the reduced mass of the ion and neutral reactant [$\mu = (m_1 m_2)/(m_1+m_2)$], α = the polarizability of the neutral molecule, which can be calculated[47] or, in some cases, values are available in the literature, μ_D = the dipole moment of the neutral reactant (values obtained from experimental literature), C = the dipole locking constant,[48] k = the Boltzmann constant, and T = the absolute temperature (298K). If the dipole moment of the neutral reactant is unknown, the Langevin collision limited rate constant (k_{Lan}) is calculated by using eq 26.[45,46]

$$k_{Langevin} = 2\pi q(\alpha/\mu)^{1/2} \qquad (26)$$

The reaction efficiences reported in this paper are the fraction of collisions between the ion and neutral reactant which result in formation of product. The efficiences are calculated by dividing k_{total} by k_{ADO} or k_{Lan} (eq 27). k_{Lan} is only calculated and used if μ_D of the neutral is unknown.

$$\text{Reaction Efficiency} = k_{total}/k_{ADO} \quad \text{(For known } \mu_D\text{)}$$
$$= k_{total}/k_{Lan} \quad \text{(For unknown } \mu_D\text{)} \qquad (27)$$

The helium used as a buffer gas was of 99.99% purity and was supplied by either Welders Products or Brown Welders Supply. The dimethyl phosphite (99.9+% pure) was obtained from Aldrich. The gas and liquid neutral reagents were obtained from commerical suppliers (Fisher, PCR, Aldrich, Matheson, and Pennwalt). The liquid substrates were fractionally distilled with a constant boiling, center cut used for the experiments. The liquids were further subjected to freeze-pump-thaw cycles to remove volatile gases before loading into the glass storage bulbs. The gas substrates were used without further purification and were loaded into glass storage bulbs following at least one freeze-pump-thaw cycle.

Other bases were used to try to produce the dimethyl phosphoryl anion. $(CH_3O)_2PO^-$ reacted with OH^- to yield $(CH_3O)_2PO^-$ along with an anion at m/z 95 believed to be the product of S_N2 displacement at a CH_3 group, $(CH_3O)P(OH)O^-$. This was also the result using CH_3O^- and $C_2H_5O^-$ as the gas-phase base. Reaction with PhN^- produced only $(CH_3O)_2PO^-$ and its cluster negative ion.

IV. RESULTS AND DISCUSSION

The kinetic and product data for the ion-molecule reactions of $(CH_3O)_2PO^-$ are summarized in Table I. In all cases, clean psuedo-first-order decay plots of the log of the ion signal of $(CH_3O)_2PO^-$ (m/z 109) verses concentration of neutral reactant were obtained. The product ion distributions in Table I are based on the integrated relative ion signals obtained from the mass spectra of the reactions. It is recognized in this study that the formation of products is due to reaction of m/z 109 and $(CH_3O)_2PO^-/H(O=)P(OCH_3)_2$ (m/z 219) with the neutral reactants. the reported branching fractions are those obtained from the mass spectral data; however, these branching fractions may be in error because they may be the result of both ions m/z 109 and m/z 219 reacting.

A. Determination of the Proton Affinity (PA) of $(CH_3O)_2PO^-$.

Initial studies were directed towards determining the proton affinity (PA) of $(CH_3O)_2PO^-$ which was accomplished using the bracketing method. Potential proton donors of known gas-phase acidity (ΔH^o_{acid} (HA)) were added to the flow containing $(CH_3O)_2PO^-$, m/z 109. Proton transfer was judged to have occurred by attenuation of the m/z 109 signal and formation of the signal for A^-. Table II summarizes the reactions used to bracket PA ($(CH_3O)_2PO^-$). The reaction of $(CH_3O)_2PO^-$ with c-C_5H_6 (reaction 26, Table I) gave exclusively the proton transfer product, c-$C_6H_5^-$.

The slow reaction of $(CH_3O)_2PO^-$ with C_2H_5SH (reaction 19, Table I) was more complex and produced five product negative ions, $C_2H_5S^-$ (m/z 61; 4%), $C_2H_5S^-/HSC_2H_5$ (m/z 123; 10%), $(CH_3O)P(H)O_2^-$ (m/z 95; 48%),

TABLE I. Summary of the Kinetic and Product Data for the Ion-Molecule Reactions of $(CH_3O)_2PO^-$ with Neutral Molecules.

RXN NO.	NEUTRAL REACTANT		PRODUCT ION + [ASSUMED NEUTRAL]	FRACTION OF PRODUCT	k_{total} cm^3 $molecule^{-1}$ s^{-1}	k_{ADO}	EFFICIENCY OF REACTION
1	CH_3Cl	-->	No Reaction		$<10^{-13}$		
2a	CH_3Br	-->	Br^- + $[(CH_3O)_2P(=O)CH_3]$	0.33	9.8×10^{-13}	1.2×10^{-9}	8.2×10^{-4}
2b		-->	$(CH_3O)_2P(=O)H/Br^-$	0.67			
3	CH_3I	-->	I^- + $[(CH_3O)_2P(=O)CH_3]$	1.00	3.0×10^{-11}	1.1×10^{-9}	0.027
4	CF_3Cl	-->	No Reaction		$<10^{-13}$		
5a	CF_3Br	-->	Br^- + $[(CH_3O)_2PO]$ + $[CF_3]$	0.06	3.2×10^{-10}	5.8×10^{-10}	0.55
5b		-->	$(CH_3O)P(Br)O_2^-$ + $[CH_3CF_3]$	0.94			
6a	CF_3I	-->	I^- + $[(CH_3O)PO]$ + $[CF_3]$	0.15	5.9×10^{-10}	9.4×10^{-10}	0.63
6b		-->	$(CH_3O)P(I)O_2^-$ + $[CH_3CF_3]$	0.85			

...d Product Data for the Ion-Molecule Reactions of $(CH_3O)_2PO^-$

...ont).

... + $[(CH_3O)_2P(O)Br]$	0.22	2.5×10^{-10}	9.5×10^{-10}	0.26
... + $[CH_3CCl_3]$	0.54			
... + $[(CH_3O)_2P(O)Cl]$	0.24			
... $HCCl_3$	1.00	4.2×10^{-11} a	1.1×10^{-9}	0.038
... + $[(CH_3O)_2P(O)Cl]$	0.81	5.1×10^{-11}	9.5×10^{-10}	0.054
... Cl^- + $[CCl_3CH_3]$	0.19			
... ClF^- + $[(CH_3O)_2P(Cl)(=O)]$	0.79	1.8×10^{-11}	9.4×10^{-10}	0.019
... $(CH_3O)P(Cl)O_2^-$ + $[CCl_2FCH_3]$	0.17			
... Cl^- + $[(CH_3O)_2P(=O)CCl_2F]$	0.04			
... $(CH_3O)P(Cl)O_2^-$ + $[CClF_2CH_3]$	0.43	1.1×10^{-12}	1.0×10^{-9}	1.1×10^{-3}
... $(CH_3O)_2P(=O)H/Cl^-$ + $[(CH_3O)_2P(O)CClF_2]$	0.57			

TABLE I. Summary of the Kinetic and Product Data for the Ion-Molecule Reactions of $(CH_3O)_2PO^-$ with Neutral Molecules (cont).

12a	CCl_2FCClF_2	--> $(CH_3O)P(Cl)O_2^-$ + $[CCl_2FCF_2CH_3]$	0.14	2.6×10^{-10}	6.1×10^{-10}	0.43
12b		--> $(CH_3O)_2P(=O)H/Cl^-$ + $[(CH_3O]_2P(O)CF_2CCl_2F]$	0.86			
13	$CHClF_2$	$\xrightarrow{He}$ $(CH_3O)_2PO^-/HCClF_2$	1.00	5.4×10^{-12} a	9.0×10^{-10}	6.0×10^{-3}
14	CH_2Cl_2	$\xrightarrow{He}$ $(CH_3O)_2PO^-/H_2CCl_2$	1.00	1.1×10^{-12} a	1.3×10^{-9}	8.5×10^{-4}
15	CO_2	$\xrightarrow{He}$ $(CH_3O)_2PO^-/CO_2$	1.00	6.2×10^{-13} a	6.6×10^{-10}	9.4×10^{-4}
16	SO_2	$\xrightarrow{He}$ $(CH_3O)_2PO^-/SO_2$	1.00	5.6×10^{-10} a	1.1×10^{-9}	0.51
17a	H_2S	$\xrightarrow{He}$ $(CH_3O)_2P(=O)H/^-SH$	0.67	2.5×10^{-10} a	1.2×10^{-9}	0.21
17b		--> $(CH_3O)P(H)O_2^-$ + $[CH_3SH]$	0.23			
17c		--> $(CH_3O)_2POH/H(O)_2P(OCH_3)^-$	0.10			
18a	CH_3SH	--> $(CH_3O)P(H)O_2^-$ + $[CH_3SCH_3]$	0.61	5.2×10^{-13}	1.3×10^{-9}	4.0×10^{-4}
18b		--> $(CH_3O)P(H)O_2^-/H(O=)P(OCH_3)_2$	0.39			

TABLE I. Summary of the Kinetic and Product Data for the Ion-Molecule Reactions of $(CH_3O)_2PO^-$ with Neutral Molecules (cont).

19a	C_2H_5SH --> $C_2H_5S^-$ + $[(CH_3O)_2P(=O)H]$	0.04	1.8×10^{-12}	1.3×10^{-9}	1.4×10^{-3}
19b	--> $C_2H_5SH/SC_2H_5^-$	0.10			
19c	--> $(CH_3O)P(H)O_2^-$ + $[C_2H_5SCH_3]$	0.48			
19d	--> $(CH_3O)_2PO/HSC_2H_5^-$	0.10			
19e	--> $(CH_3O)P(H)O_2^-/H(O=)P(OCH_3)_2$	0.28			
21	CH_3NO_2 $\xrightarrow{He}$ $(CH_3O)_2PO^-/CH_3NO_2$	1.00	6.7×10^{-12} a	2.1×10^{-9}	3.2×10^{-3}
22	CF_3CH_2OH $\xrightarrow{He}$ $(CH_3O)_2PO^-/HOCH_2CF_3$	1.00	Not measured		
23a	$(CF_3)_2C=O$ --> $(CH_3O)_2P(=O)C(CF_3)_2O^-$	0.17	5.4×10^{-10}	1.1×10^{-9}	0.49
23b	--> $CH_3OP(O)(CF_3)^-$ + $[CH_3C(O)CF_3]$	0.50			
23c	--> $CH_3OC(CF_3)_2O^-$ + $[CH_3OP=O]$	0.33			
23d	--> $(CF_3)_2PO^-$ (secondary product)				
23e	--> $(CH_3O)(CF_3)P(O)/C(O)(CF_3)_2^-$ (secondary product)				

TABLE I. Summary of the Kinetic and Product Data for the Ion-Molecule Reactions of $(CH_3O)_2PO^-$ with Neutral Molecules (cont).

24	$(CH_3)_2C{=}O \rightarrow (CH_3O)_2POC(CH_3)_2O^-$	1.00	1.0×10^{-13} b	1.7×10^{-9}	5.9×10^{-5}
25a	$CF_3CO_2CH_3 \xrightarrow{He} (CH_3O)_2PO^-/CF_3CO_2CH_3$	0.09	4.6×10^{-12} a	1.5×10^{-9}	3.1×10^{-3}
25b	$\rightarrow CF_3CO_2^- + [(CH_3O)_2P(=O)CH_3]$	0.91			
26a	$CF_3CO_2C_2H_5 \xrightarrow{He} (CH_3O)_2PO^-/CF_3CO_2C_2H_5$	0.12	6.0×10^{-12} a	1.5×10^{-9}	4.0×10^{-3}
26b	$\rightarrow CF_3CO_2^- + [(CH_3O)_2P(=O)C_2H_5]$	0.88			
27	$o\text{-}C_5H_6 \rightarrow o\text{-}C_5H_5^- + [(CH_3O)_2P(=O)H]$	1.00	Not measured		
28	$(NC)_2C{=}C(CN)_2 \rightarrow (NC)_2C{=}C(CN)_2^- + [(CH_3O)_2PO]$	1.00	Not measured		
29	$o\text{-}ClC_6H_4CF_3 \xrightarrow{He}$ adduct	1.00	Not measured		
30	$p\text{-}BrC_6H_4CF_3 \rightarrow$ No Reaction				
31	$m\text{-}BrC_6H_4CF_3 \rightarrow$ No Reaction				
32	$o\text{-}BrC_6H_4CF_3 \xrightarrow{He}$ adduct	1.00	Not measured		

TABLE I. Summary of the Kinetic and Product Data for the Ion-Molecule Reactions of $(CH_3O)_2PO^-$ with Neutral Molecules (cont).

33	p-$(O_2N)_2C_6H_4$	-->	No Reaction	
34	2,3-dichloro-1,4-naphthoquinone	-->	No Reaction	
35	NO_2	-->	NO_2^-	Not measured

[a]Apparent bimolecular rate constant for termolecular process. [b]Kinetic data at 1.00 torr only.

TABLE II. Summary of Proton Affinity Bracketing Reactions for $(CH_3O)_2PO^-$.

HA	H^+ - TRANSFER	$\Delta H^o_{acid}(HA)^{a,b}$ (kcal/mol)
H_2S	yes	353.4
$\underline{c}$-C_5H_6	yes	356.1
C_2H_5SH	yes	357.5
CH_3NO_2	no	358.7
CH_3SH	no	359.0
CF_3CH_2OH	no	364.4

[a] $\Delta H^o_{acid}(HA)$ values obtained from J.E. Bartmas, R.T. McIver, "The Gas-Phase Acidity Scale" in "Gas Phase Ion Chemistry," Bowers, M.T., Ed.; Acedemic Press: New York, 1979; Vol.2, Chapter 11. [b] Errors are $\pm$ 2 kcal/mol.

$(CH_3O)_2P(=O)H/^-SC_2H_5$ (m/z 171; 10%), and $(CH_3O)_2P(=O)H/^-O_2P(H)(OCH_3)$ (m/z 205; 28%). The ions m/z 123 and 171 containing one and two sulfur atoms, respectively, were readily assigned based on their (M + 2) isotope peaks due to ^{34}S. However, the signal for m/z 61 was too small

to use this method. The isotope (M + 1) ratio for m/z 95 (obs. 1.3%; theory 1.1%) is in reasonable agreement with its structural assignment. Again the signal for m/z 205 was too small to use this method to verify the structure. Formation of these ions can be interpreted from an initial slightly exothermic proton transfer between $(CH_3O)_2PO^-$ and C_2H_5SH from the single excited complex $\underline{1}^*$ shown in Scheme I.

Scheme I

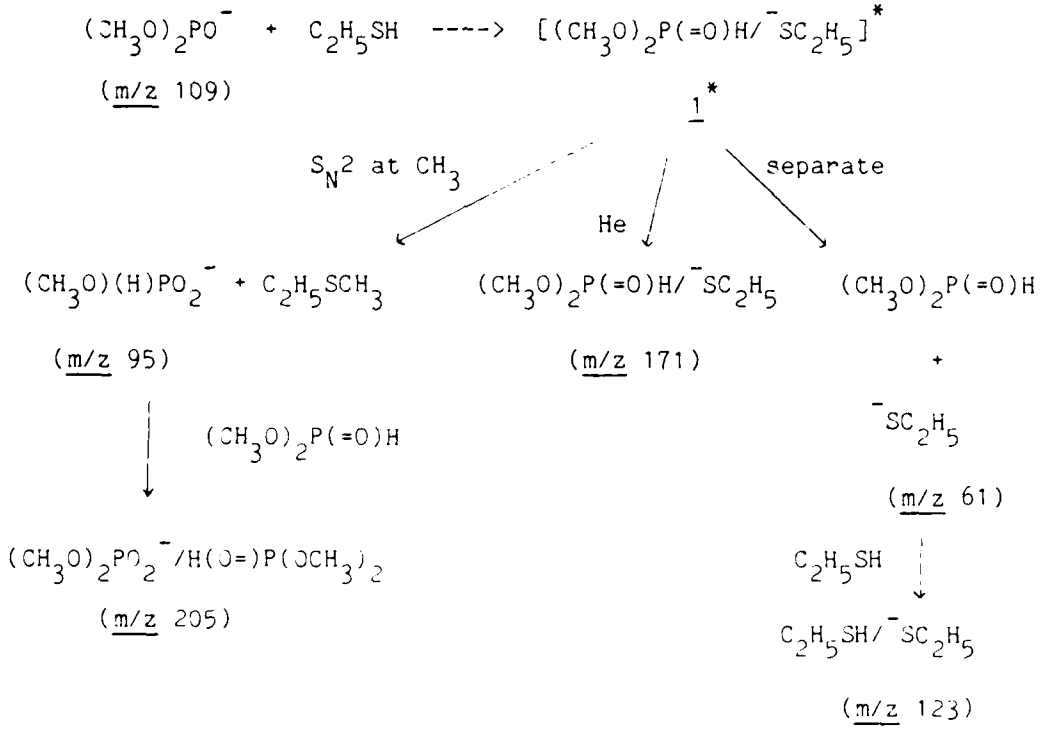

Once the initial proton transfer occurs in the excited complex $\underline{1}^*$, there are three different reaction pathways that are followed to produce the observed ion products. The excited complex may separate into a neutral plus m/z 61 which is the expected product from proton transfer. The excited complex may be stabilized through collision with the helium

buffer gas giving the cluster ion, m/z 171. Finally, while still in the complex, $C_2H_5S^-$ may attack at a methyl group giving S_N2 displacement and producing $(CH_3O)(H)PO_2^-$ at m/z 95. The latter product ion can form the cluster ion with excess $(CH_3O)_2P(=O)H$ in the flow tube giving a hydrogen bonded adduct ion observed at m/z 205.

The very slow reaction of $(CH_3O)_2PO^-$ with CH_3SH (reaction 18, Table I) produced only the two negative ions $(CH_3O)P(H)O_2^-$ (m/z 95) and its H-bonded cluster $(CH_3O)P(H)O_2^-/H(O=)P(OCH_3)_2$ (m/z 205). The production of the ion m/z 95 suggests that the H^+ transfer from CH_3SH to $(CH_3O)_2PO^-$ is somewhat endothermic but may occur within the attractive excited ion-neutral complex $[(CH_3O)_2PO^-/HSCH_3]^*$ giving $[(CH_3O)_2P(=O)H/^-SCH_3]^*$. The latter complex cannot separate due to the endothermicity of the H^+ transfer, but, apparently, is able to effect S_N2 displacement by CH_3S^- on a CH_3-group of the phosphite yielding the observed ion m/z 95. This is analogous to the major product channel in the reaction of $(CH_3O)_2PO^-$ with C_2H_5SH. Further clustering of m/z 95 with excess $(CH_3O)_2P(=O)H$ present in the flow yields m/z 205.

In the reaction of $(CH_3O)_2PO^-$ with H_2S (reaction 17, Table I) the formation of three products was observed, $HS^-/H(O=)P(OCH_3)_2$ (m/z 143, 67%), $(CH_3O)P(H)O_2^-$ (m/z 95, 23%), and $(CH_3O)_2P(=O)H/^-O_2P(H)(OCH_3)$ (m/z 205, 10%). The product m/z 143 was characterized by its (M + 2) isotope peak indicating the presence of one S atom. In this reaction, the proton transfer from H_2S to $(CH_3O)_2PO^-$ is rapid. The resulting HS^- then rapidly clusters with neutral $(CH_3O)_2P(=O)H$ to produce m/z 143. HS^- can also attack at a CH_3-group to give the S_N2 displacement product, m/z 95. This product then clusters with $(CH_3O)_2P(=O)H$ to form the product m/z 205.

The reaction of CH_3NO_2 with $(CH_3O)_2PO^-$ (reaction 21, Table I) resulted in no proton transfer product but, rather the slow formation of a cluster ion, $(CH_3O)_2PO^-/CH_3NO_2$. Similiar clustering occurred with CF_3CH_2OH (reaction 22, Table I). This is probably the hydrogen-bonded adduct anion.

From the results in Table II, $PA((CH_3O)_2PO^-) = 358 \pm 2$ kcal/mol; assuming that the proton transfer occurs at phosphorus, $\Delta H^\circ_{acid}((CH_3O)_2P(=O)H) = PA((CH_3O)_2PO^-)$. This is in excellent agreement with the reported value of 357 ± 3 kcal/mol obtained from studies by DePuy and co-workers.[5]

Benson's Tables[49] were used to calculate thermochemical values for dimethyl phosphonate, $\Delta H^\circ_f((CH_3O)_2P(=O)H) = -198.1$ kcal/mol. From eq 28 for the ionization of $(CH_3O)_2P(=O)H$, one can calculate

$$(CH_3O)_2P(=O)H \xrightarrow{\Delta H^\circ_{acid}} (CH_3O)_2PO^- + H^+ \qquad (28)$$

$\Delta H^\circ_f((CH_3O)_2PO^-) = -207.3 \pm 2$ kcal/mol. This value can then be used to calculate ΔH° for reactions with $(CH_3O)_2PO^-$.

B. Determination of Electron Affinity (EA) of $(CH_3O)_2P(=O)^\cdot$.

The bracketing technique was also used to determine the electron affinity of $(CH_3O)_2P(=O)^\cdot$. Neutral substrates of known electron affinity were introduced into the flow containing $(CH_3O)_2P(=O)^\cdot$. Electron transfer was judged to have occurred by attenuation of the m/z 109 signal and formation of the signal for the anion radical of the neutral molecule. Table III summarizes the reactions used to accomplish this determination. No reaction was observed with 2,3-dichloro-1,4-naptnoquinone whereas reaction with tetracyanoethylene produced

TABLE III. SUMMARY OF ELECTRON AFFINITY BRACKETING REACTIONS FOR $(CH_3O)_2P(=O)^{\bullet}$.

NEUTRAL	EA OF NEUTRAL	ELECTRON TRANSFER
p-Dinitrobenzene	1.89 eV[a]	no
2,3-Dichloro-1,4-naphthoquinone	2.08 eV[a]	no
$(NC)_2C=C(CN)_2$	2.3 eV[b]	yes
NO_2	2.31eV[a]	yes

[a]EA values obtained from Grimsrud, E.P.; Caldwell, G.; Chowdhury, S.; Kebarle, P. J. Am. Chem. Soc., 1985, 107, 4627-4634. [b]Janousek, B.K.; Brauman, J.I. In "Gas Phase Ion Chemistry," Bowers, M.T., Ed.; Acedemic Press: New York, 1979; Vol.2, Chapter 10.

exclusively the product of electron transfer, $(NC)_2C=C(CN)_2^-$ (m/z 128). Therefore, EA($(CH_3O)_2P(=O)^{\bullet}$) = 2.2 $\pm$ 0.1 eV.

C. Reactions of $(CH_3O)_2PO^-$ with the Methyl Halides.

To determine the intrinsic S_N2 kinetic nucleophilicity of $(CH_3O)_2PO^-$, the reactions of this anion with the methyl halides, CH_3X, were investigated with the results listed in Table I (See reactions 1-3). The rates of these reactions ranged from moderate with CH_3I (eq 29)

TABLE IV. ΔH^{o}_{rxn} for the Reaction of $(CH_3O)_2PO^-$ with Methyl Halides.

METHYL HALIDE	$\Delta H^{o}_{rxn}((CH_3O)_2P(=O)CH_3)^a$ kcal/mol	$\Delta H^{o}_{rxn}((CH_3O)_3P)^a$ kcal/mol	k_{total} cm^3/molecule-s
CH_3I	-52.2	-9.3	3.0×10^{-11}
CH_3Br	-45.6	-2.7	9.5×10^{-13}
CH_3Cl	-37.7	+5.2	$<10^{-13}$

[a]Calculated using thermodynamic data from ref 49.

to slow with CH_3Br (eq 30) to no observed reaction with CH_3Cl. In addition to the S_N2 product, Br^-, clustering of Br^- with excess netrual $(CH_3O)_2P(=O)H$ was observed yeilding the ion m/z 159,161. The two peaks were of the same intensity which is characteristic of the (M + 2) isotope ratio for Br^-.

$$(CH_3O)_2PO^- + CH_3I \longrightarrow I^- + \text{[illegible]} \quad (29)$$

or

$$\text{[illegible]}$$

$$(CH_3O)_2PO^- + CH_3Br \xrightarrow{\underline{0.33}} Br^- + \text{[illegible]} \quad (30)$$

$$\xrightarrow{\underline{0.67}} Br^-\cdot H(=O)P(OCH_3)_2$$

(m/z 159,161)

The phosphoryl anion is an ambident species with possible reactive sites at oxygen or phosphorus. The reactions of $(CH_3O)_2PO^-$ with the methyl halides indicates that the phosphoryl anion is kinetically a poor nucleophile in S_N2 displacement reactions. Experiments on the reactivity of PO_3^- in the gas-phase[28] also showed that this phosphorus anion is a relatively unreactive species.

The neutral product formed in the reaction of $(CH_3O)_2PO^-$ with these methyl halides has two possible isomeric structures. The ΔH_f^o of the two neutral tautomers $\Delta H_f^o((CH_3O)_2P(=O)CH_3)$ = -210.2 kcal/mol and $\Delta H_f^o((CH_3O)_3P)$ = -167.6 kcal/mol differ by 43 kcal/mol. It was not possible to identify which tautomer neutral was formed in these S_N2 reactions. The methyl transfer could have occured at phosphorus under themodynamic control where a large intrinsic barrier exists or it could have occurred at oxygen under kinetic control with a smaller intrinsic barrier. A much lower reaction exothermicity exists with the methyl transfer occuring at oxygen. Table IV compares the ΔH_{rxn}^o for the two possible tautomers formed from the reaction of $(CH_3O)_2PO^-$ with the methyl halides. From the evaluation of the thermochemical data, it is probable that the structure of the neutral formed in this reaction is the phosphonate tautomer.

D. Reactions of $(CH_3O)_2PO^-$ with Polyhalogenated Alkanes.

In an attempt to investigate and model the initial electron transfer step in the $S_{RN}1$ mechanism, $(CH_3O)_2PO^-$ was allowed to react with CF_3X where X = I, Br, Cl. The reactions with CF_3I (eq 31) and CF_3Br (eq 32) were fast while no reaction was observed with CF_3Cl (see reactions 4-6, Table I).

$$(CH_3O)_2PO^- + ICF_3 \begin{cases} \xrightarrow{0.15} I^- + (CH_3O)_2PO + CF_3 \\ \xrightarrow{0.85} (CH_3O)(I)PO_2^- + CF_3CH_3 \\ \quad (\underline{m/z}\ 221) \end{cases} \quad (31)$$

$$(CH_3O)_2PO^- + BrCF_3 \begin{cases} \xrightarrow{0.06} Br^- + (CH_3O)_2PO + CF_3 \\ \xrightarrow{0.94} (CH_3O)(Br)PO_2^- + CF_3CH_3 \\ \quad (\underline{m/z}\ 173) \end{cases} \quad (32)$$

In the reaction with ICF_3, the product $\underline{m/z}$ 221 was characterized by the (M + 1) isotope peak (obs. 1.9%, theory 2.2%). The products in the reaction with CF_3Br were characterized through their (M + 2) isotope peak which is of equal intensity to $\underline{m/z}$ 79 and $\underline{m/z}$ 173 indicating that one Br atom is present in each product ion. The major product of these reactions was the transfer of the halogen atom to and loss of a methyl group from $(CH_3O)_2PO^-$; the major product structures are considered to be 8. A similiar product is seen in the condensed phase in the reaction of halogen molecules with phosphorus compounds containing an alkoxy group (eq 33).[2]

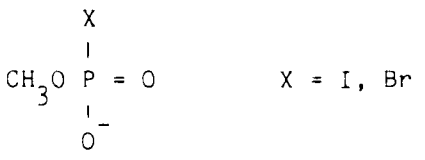

X = I, Br

8

$$(RO)_2POR' + X_2 \longrightarrow (RO)_2P(=O)X + R'X \quad (33)$$

The efficiency of the two reactions of $(CH_3O)_2PO^-$ with CF_3I and CF_3Br are about equally high with reaction occurring in approximately six out of every ten collisions. No reaction was observed with $ClCF_3$

indicating that this rate constant is less than the lower limit of detection in the FA, $\leq 10^{-13}$ cm^3 $molecule^{-1}$ s^{-1}.

This drastic change in rate constants between $BrCF_3$ and $ClCF_3$ is not in keeping with simple halogen atom transfer. Since the C-X bonds and the P-X bonds should show a closer parrallel relationship, no such sharp break in rate should be exhibited if the mechanism involves only simple halogen atom transfer. However, this discontinuity would be expected if the reaction mechanism involved initial electron transfer and the electron affinity (EA) of $ClCF_3$ is too small to allow this step to occur. Electron affinities for halogenated alkanes used in this study are listed in Table V.

TABLE V. ELECTRON AFFINITIES FOR SELECTED HALOGENATED ALKANES

RX	EA (eV)	RX	EA (eV)
CCl_4	2.06[a]	CCl_2FCClF_2	-
$CHCl_3$	1.7[a]	CF_3I	1.57[d,e]
CH_2Cl_2	1.31[a]	CF_3Br	0.97[d,e]
CF_2Cl_2	0.4[b,c]	CF_3Cl	-0.4[f]
$CFCl_3$	1.1[b,c]	$CHClF_2$	-0.96[f]
CCl_3Br	-		

[a]Gaines, A.F.; Day, J.; Page, F.M. Trans. Faraday Soc., 1966, 62, 874. [b]Dispert, H.; Lackmann, K. Int. J. of Mass Spec. and Ion Phys., 1978, 28, 49-67. [c]Error ± 0.3 eV. [d]See ref 43 [e]Error ± 0.2 eV. [f]See ref 53.

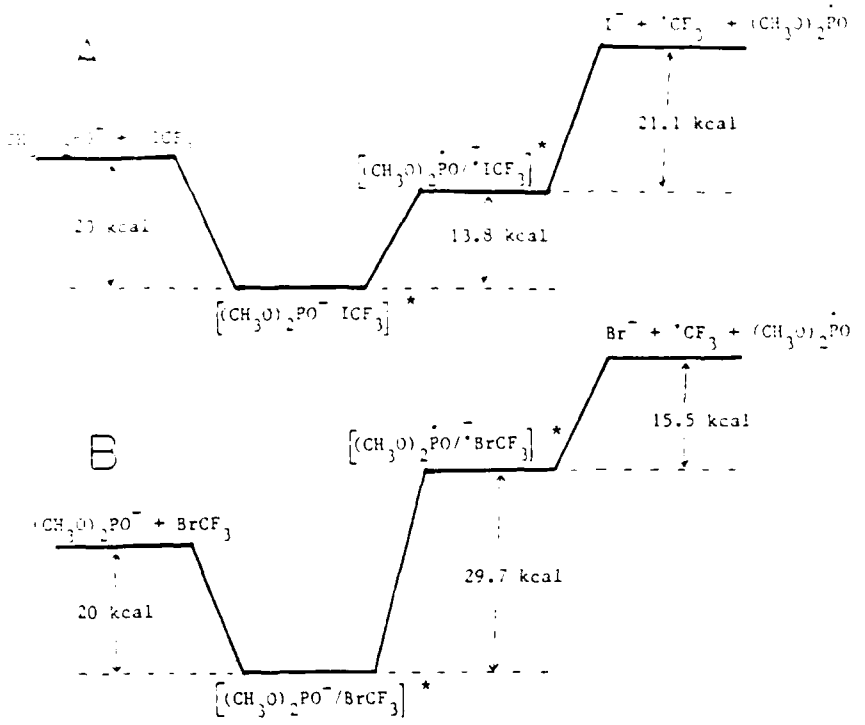

Figure 4. Energy level diagrams for electron transfer and fragmentation in the reaction of $(CH_3O)_2PO^-$ with (A) ICF_3 and (B) $BrCF_3$.

The enthalpy diagrams in Figure 4 clearly illustrate the point that the formation of I^- and Br^- from the fast reactions of $(CH_3O)_2PO^-$ with ICF_3 and $BrCF_3$, respectively, cannot occur by simple electron transfer followed by fragementation of XCF_3^-. In a search for a mechanism process to account for these reactions, attention was focused on the structures of the neutral product of the electron transfer, the radical

$(CH_3O)_2\dot{P}=O$ and the ion product of halide ion transfer, $(CH_3O)(X)PO_2^-$. The dimethoxy phosphoryl radical could undergo radical β-fragmentation yielding methyl metaphosphate $(CH_3O)PO_2$ and a methyl radical. This fragmentation would be more exothermic if it was instigated by $F_3C^\cdot$ so that the product would be CF_3CH_3 rather than $^\cdot CH_3$ (eq 34). The methyl metaphosphate would be expected to add X^- within the collision complex to give the major product of these reactions (eq 35).

$$F_3C^\cdot + (CH_3O)_2\dot{P}=O \longrightarrow F_3C\text{-}CH_3 + (CH_3O)PO_2 \quad (34)$$

$$(CH_3O)PO_2 + X^- \longrightarrow (CH_3O)(X)PO_2^- \quad (35)$$

Unfortunately, the ΔH° of eq 34 cannot be calculated since $\Delta H^\circ_f((CH_3O)_2PO_2)$ is unknown and cannot even be approximated. However, ΔH°(eq 34) is expected to be reasonably exothermic since a C-O bond is lost in the phosphoryl radical while a C-C bond and a P=O bond (from a P-O bond) are generated in the products. This exothermicity must be $\geq$ 21 kcal/mol which is the $D^\circ(F_3C\text{-}I^-)$.[56]

However, similar application of ΔH°(eq 34) to the reaction of $(CH_3O)_2PO^-$ with $BrCF_3$ does not answer the question of why this reaction was also fast ($k_{total} = 3.2 \times 10^{-10}$; reaction efficiency = 0.55). Here the electron transfer is 29.7 kcal/mol endothermic. Even assuming a maximum effect of ion-dipole and ion-induced dipole forces in the collision complex of 20 kcal/mol, electron transfer remains about 10 kcal mol net endothermic in the collision complex. Even in the absence of barriers to and from the collision complex $[(CH_3O)_2\dot{P}O/^-BrCF_3]$, the reaction would not occur; however, the reaction is observed to be fast. Thus, simple electron transfer must not be the mechanism.

To circumvent this problem, it is suggested that the electron and group (CH_3 and CF_3) transfers occur concertedly via a transition state (9) with a low activation barrier to account for the overall fast reaction rate. The single barbed arrows in 9 are simply to show possible electron motion. The small amount of Br^- observed probably arises by partial fragmentation of excited $(CH_3O)(Br)PO_2^-$. The absence of electron transfer to CF_3Cl due to its negative EA shows that the reaction between $(CH_3O)_2PO^-$ and CF_3Br is not simple Br-atom transfer.

Results [illegible] may be some correlation [illegible] with $(CH_3O)_2PO^-$ [illegible].

The [illegible] produced [illegible] $CBrCl_2^-$ [illegible] 4, and M [illegible] approximately [illegible].

$$(CH_3O)_2PO^- + CCl_3Br \longrightarrow [illegible]$$

[illegible]

[illegible]

CCl_4 reacted with $(CH_3O)_2PO^-$ [illegible] slower than did CCl_3Br to produce mainly [illegible] and

$(CH_3O)P(Cl)O_2^-$ was a minor product. The efficiency of this reaction is now only 5 out of 100 collisions.

$$(CH_3O)_2PO^- + CCl_4 \begin{cases} \xrightarrow{0.81} CCl_3^- + (CH_3O)_2P(=O)Cl \\ \xrightarrow{0.19} (CH_3O)P(Cl)O_2^- + CCl_3CH_3 \end{cases} \quad (37)$$

The major product observed in the reaction with CCl_4 was the same as in the solution phase[2] (eq 9) when the dialkoxy phosphoryl anion is oxidized by CCl_4. The minor product, however, was not observed in solution.

CCl_3F reacts with $(CH_3O)_2PO^-$ (reaction 10, Table I) to form electron transfer products of CCl_2F^-, Cl^-, and $(CH_3O)P(Cl)O_2^-$ (eq 38). The products here again were characterized by their (M + 2 and M + 4) isotope peaks. The efficiency of this reaction was approximately 2 out of every 100 collisions resulting in reaction.

$$(CH_3O)_2PO^- + CCl_3F \begin{cases} \xrightarrow{0.79} CCl_2F^- + (CH_3O)_2P(Cl)(=O) \\ \xrightarrow{0.17} (CH_3O)P(Cl)O_2^- + CCl_2FCH_3 \\ \xrightarrow{0.04} Cl^- + (CH_3O)_2P(=O)CCl_2F \end{cases} \quad (38)$$

The results of the reactions of $(CH_3O)_2PO^-$ with $BrCCl_3$, CCl_4, and $CFCl_3$ were surprising mainly from the fact that trihalomethyl anions were observed as major products. These results suggest that replacing the F_3C-group in CF_3X by a Cl_3C-group in Cl_3CX or Cl_2FC-group in $CFCl_3$ either opens up a new product forming channel or that the group replacement hinders a channel available in the reactions of F_3CI and F_3CBr substrates. The former reason is suspected as the cause for this type of product ion formation since the corresponding $D^\circ(C\text{-}X)$ in the Cl_3C-X series ($D^\circ(Cl_3C\text{-}Cl)$ = 73.1 $\pm$ 1.8 kcal/mol,[59,60] $D^\circ(FCl_2C\text{-}Cl)$ = 73 $\pm$ 2 kcal/mol,[59,61] $D^\circ(Cl_3C\text{-}Br)$ = 55.3 $\pm$ 3 kcal/mol[59,62] are lower than

in the F_3C-X series ($D^o(F_3C\text{-}Cl)$ = 86.2 ± 3 kcal/mol,[59,63] $D^o(F_3C\text{-}Br)$ = 70.6 ± 3 kcal/mol[59,64].

For these three product channels in different reactions yielding the trihalomethyl anion, the overall processes involve X^+ transfer from the perhalomethane to $(CH_3O)_2PO^-$. The simplest mechanism to accomplish this is that of direct displacement by the phosphoryl anion on the X-C bond. However, the author is not aware of any literature precedent for this mechanism.

Alternatively, initial electron and halide ion transfer might then be followed by competitive demethylation and electron transfer shown in eq 39. However, at least one problem exists with this interpretation.

$$(CH_3O)_2PO^- + XCY_3 \longrightarrow (CH_3O)_2(X)P{=}O^{\cdot}/{}^{\cdot}CY_3 \qquad (39)$$

$$\swarrow \qquad \searrow$$

$$(CH_3O)(X)PO_2^- + CH_3CY_3 \qquad (CH_3O)_2(X)P{=}O + {}^-CY_3$$

That is why does this competition following electron and halide ion transfer occur with $XCCl_3$, but not with XCF_3 since $EA(F_3C^{\cdot}) \geq EA(Cl_3C^{\cdot})$.[53] At this time an answer to this question is not available. Therefore, the first mechanistic suggestion is adopted.

The reaction of $(CH_3O)_2PO^-$ with CCl_2F_2 (reaction 11, Table I) produced Cl^-, which was seen as the cluster $(CH_3O)_2P(=O)H/Cl^-$, and $(CH_3O)P(Cl)O_2^-$ (eq 40). In a separate experiment, Cl^- was produced from electron attachment to CCl_4 and then neutral $(CH_3O)_2P(=O)H$ was introduced into the flow. The cluster m/z 145 was rapidly formed as the only product. The efficiency of the reaction of $(CH_3O)_2PO^-$ with CCl_2F_2 was very poor, only 1 out of every 1000 collisions resulted in reaction.

$$(CH_3O)_2PO^- + CCl_2F_2 \begin{cases} \xrightarrow{0.57} (CH_3O)_2P(=O)H/Cl^- \\ \qquad (\underline{m/z}\ 145) \\ \xrightarrow{0.43} (CH_3O)P(Cl)O_2^- + CClF_2CH_3 \end{cases} \quad (40)$$

In the reaction of CCl_2FCClF_2 with the phosphoryl anion (reaction 12, Table I), the major product here again was Cl^-, observed as the cluster ion $\underline{m/z}$ 145, along with a small amount of $(CH_3O)P(Cl)O_2^-$ (eq 41). The efficiency of this reaction was very high with reaction occuring in approximately 4 out of every 10 collisions.

$$(CH_3O)_2PO^- + CCl_2FCClF_2 \begin{cases} \xrightarrow{0.86} (CH_3O)_2P(=O)H/Cl^- + (CH_3O)_2P(=O)CClFCClF_2 \\ \xrightarrow{0.14} (CH_3O)P(Cl)O_2^- + CH_3CClFCClF_2 \end{cases} \quad (41)$$

The results of this series of ion-molecule reactions suggested that an electron transfer process best explains the results. It was apparent, however, that no correlation between the product distribution and rates for this series of reactions and their corresponding electron affinities (Table V) could be drawn.

Through work being done by laboratory co-worker, Michael Jones, it became apparent that another parameter may be more appropriate in explaining the results obtained in this latter series of kinetic experiments with polyhalomethanes. Jones observed that the rates of reaction of transition metal carbonyl anions with polyhalogenated alkanes may be correlated to the thermal electron attachment rate constants (k_{TEA}) of the polyhalogenated alkane. The k_{TEA}s for the neutrals used in this study are listed in Table VI and Figure 5 shows the plot of log (k_{TEA}) verses log (k_{obs}) for the five polyhaloalkanes reacting with $(CH_3O)_2PO^-$.

TABLE VI. Thermal Electron Attachment Data.

ALKANE	k_{TEA}	k_{total} cm^3 $molecule^{-1}$ s^{-1}
CCl_4	$3.9x10^{-7}$ [a]	$5.1x10^{-11}$
$CFCl_3$	$2.6x10^{-7}$ [a]	$1.8x10^{-11}$
CCl_2FCClF_2	$3.5x10^{-8}$ [b]	$2.6x10^{-10}$
CCl_2F_2	$3.2x10^{-9}$ [a]	$1.1x10^{-12}$
CF_3Br	$1.6x10^{-8}$ [c]	$3.2x10^{-10}$

[a] See ref 65. [b] Blaustein, R. P.; Christophorou, L. G. J. Chem. Phys., 1968, 49, 1526. [c] Alge, E.; Adams, N. G.; Smith D. J. Phys. B: At. Mol. Phys., 1984, 17, 3827-3833.

The plot in Figure 5 shows only a poor correlation of the five-point data set in Table VI. A reasonable correlation is found for the three reactions of $(CH_3O)_2PO^-$ with CCl_4, $CFCl_3$, and CF_2Cl_2 with k_{total} decreasing as k_{TEA} of the polyhalomethane decreases. However, based on this parital correlation, the k_{total}s for both CCl_2FCClF_2 and CF_3Br are considerable larger than they should be. The k_{TEA} for CCl_2FCClF_2 is questionable since it was determined by a different group much earlier in the development of these rate constants. The same argument, however, cannot be applied to k_{TEA} for CF_3Br since it was recently reported by the Smith and Adams group.

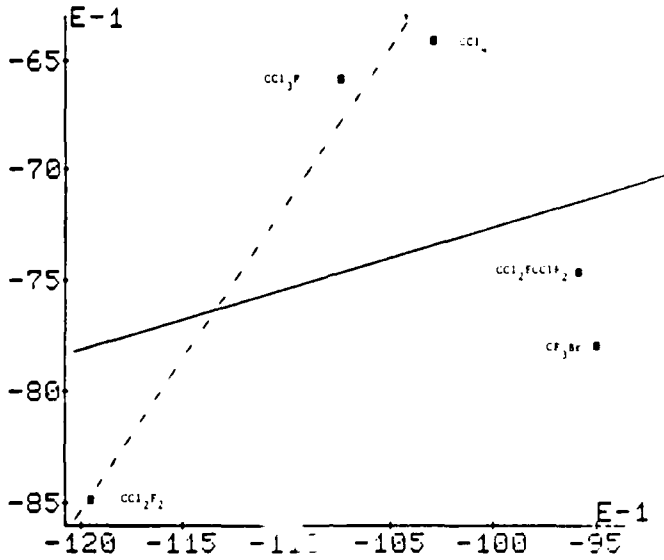

Figure 5. Plot of log (k_{TEA}) verses log (k_{obs}). (Solid line represents correlation of all points and dashed line only CCl_4, CCl_2F_2, CCl_3F.)

The suggestion that the mechanism of the reactions of $(CH_3O)_2PO^-$ with polyhalomethanes occurs by initial electron transfer is still considered valid. However, the nature of the correlating function (or mixture of functions) of the polyhalomethanes is not established by the present study. Unfortunately, the existing data set is too limited. This was futher complicated by observation of total adduct formation in the reactions of $(CH_3O)_2PO^-$ with $HCCl_3$, $HCClF_2$, and H_2CCl_2 discussed in the next section.

E. Reactions of $(CH_3O)_2PO^-$ with Halogenated Methanes Containing Hydrogen.

Reaction of $(CH_3O)_2PO^-$ with $CHCl_3$ (reaction 8, Table I), $CHClF_2$ (reaction 13, Table I), and CH_2Cl_2 (reaction 14, Table I) resulted in tne formation of the total adducts (eq 42-44). The efficiency of these

reactions are low, 4 out of 100 collisions for $CHCl_3$, 6 out of 1000 for $CHClF_2$, and 9 out of 10,000 for CH_2Cl_2. The product ions were characterized by the isotope peaks for three, one, and two chlorine atoms respectively.

$$(CH_3O)_2PO^- + CHCl_3 \xrightarrow{He} (CH_3O)_2PO^-/HCCl_3 \quad (42)$$

$$(CH_3O)_2PO^- + CHClF_2 \xrightarrow{He} (CH_3O)_2PO^-/HCClF_2 \quad (43)$$

$$(CH_3O)_2PO^- + CH_2Cl_2 \xrightarrow{He} (CH_3O)_2PO^-/HCHCl_2 \quad (44)$$

In this particular series of halogenated methanes, it appears that the driving force for reaction is the formation of a hydrogen bonded species rather than reaction through an electron transfer process. Literature has provided a number of examples of hydrogen bonded ion species in the gas phase.[4,27,28] The electron affinity of these methanes (Table IV) ranges from high for $CHCl_3$ and CH_2Cl_2 to a negative electron affinity for $CHClF_2$. The k_{TEA}s for these compounds ($k_{TEA}(CHCl_3) = 4.2 \times 10^{-11}$;[65] $k_{TEA}(CH_2Cl_2) = 4.8 \times 10^{-11}$;[66] $k_{TEA}(CHClF_2) = <1.6 \times 10^{-15}$[53]) are very small and the rates of reaction for an electron transfer process similar to that which is occurring in CCl_4, $CFCl_3$, and CF_2Cl_2 would lie well below the lower limit of detection of the FA system. Since species of lower electron affinity than $CHCl_3$ and CH_2Cl_2 reacted through a electron transfer process, it may be suggested that the hydrogen bonding in these halogenated methanes with a hydrogen is a stronger ion-neutral attraction than is the electron transfer.

It has been suggested[28] that the rates of formation of clusters for this type of reaction may be correlated to the relative acidities of the neutral molecules. The gas phase acidities of these compounds are not all known. However, from the fact that $\Delta H^\circ_{acid}(CHCl_3) = 362 \pm 6$

kcal/mol[54] and $\Delta H^{o}_{acid}(CHF_3)$ = 375 kcal/mol[54], it appears that as a chlorine is replaced by a fluorine, the acidity decreases. This would be in line with the ordering of observed rate constants (Table I) which show $CHCl_3$ > $CHClF_2$ > CH_2Cl_2. This is reasonably the decreasing order of acidity for these compounds in the gas phase; however, their gas-phase acidities are unknown.

F. Reactions of $(CH_3O)_2PO^-$ with SO_2 and CO_2.

$(CH_3O)_2PO^-$ reacted with both of these neutrals to form the total adduct. The very slow reaction with CO_2 (reaction 15, Table I) gave exclusively the total adduct at m/z 157 (eq 45). The fast reaction with SO_2 (reaction 16, Table I) produced a similar product at m/z 173 (eq 46). The product at m/z 173 had the characteristic (M + 2) isotope peak for the presence of one sulfur atom.

In these reactions, the phosphoryl anion attacks the carbonyl or sulfonyl center as a nucleophile producing a total adduct anion, which requires termolecular collisional stabilization with the buffer gas.

$$(CH_3O)_2PO^- + CO_2 \xrightarrow{He} \underset{m/z\ 157}{(CH_3O)_2P(=O)CO_2^-} \quad (45)$$

$$(CH_3O)_2PO^- + SO_2 \xrightarrow{He} \underset{m/z\ 173}{(CH_3O)_2P(=O)SO_2^-} \quad (46)$$

The nature of the bonding (to P or O) in these adducts is unknown. The faster rate of the reaction with SO_2 was expected due to the Lewis acidity of SO_2. These reactions showed no pressure dependence when conducted at 0.5 torr and 1.0 torr for SO_2 and 0.4 torr and 1.0 torr for CO_2.

G. Reactions of $(CH_3O)_2PO^-$ with Ketones.

When $(CH_3O)_2PO^-$ was allowed to react with $(CF_3)_2C{=}O$ (reaction 23, Table I), the primary product ions were the total adduct, a product resulting from replacement of one CH_3O-group by a CF_3-group in the dimethoxy phosphoryl anion, and a negative ion at m/z 197 which is postulated to be structure 9 (eq 47). The m/z 147 ion reacted further with $(CF_3)_2C{=}O$ (eq 48) to form the total adduct plus a product ion at

$$(CH_3O)_2PO^- \ (m/z\ 109) + (CF_3)_2C{=}O \xrightarrow{0.50} (CH_3O)(CF_3)PO^- \ (m/z\ 147) + CH_3OC(=O)CF_3$$
$$\xrightarrow{0.33} (CH_3O)(CF_3)_2CO^- \ (m/z\ 197)$$
$$\xrightarrow{0.17} (CH_3O)_2P(=O)C(CF_3)_2O^- \ (m/z\ 275) \qquad (47)$$

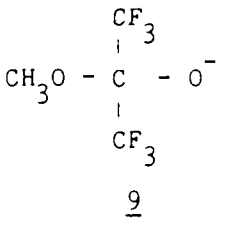

9

m/z 185 believed to be $(CF_3)_2PO^-$ where both CH_3-groups in the starting phosphoryl anion have been replaced by CF_3-groups.

$$(CH_3O)P(CF_3)O^- \ (m/z\ 147) + (CF_3)C{=}O \longrightarrow (CF_3)_2PO^- \ (m/z\ 185) + CF_3CO_2CH_3$$
$$\longrightarrow (CH_3O)P(CF_3)OC(CF_3)_2O^- \ (m/z\ 313) \qquad (48)$$

The isotope (M + 1) peak ratios for m/z 147 (obs 2.8%, theory 2.2%), 185 (obs 2.2%, theory 2.2%), 197 (obs 3.3%, theory 4.4%), 275

(obs 5.2, theory 5.5%), and 313 (obs 6.1%, theory 5.5%) are in reasonable agreement with suggested structures. The efficiency of reaction 47 was high with reaction occuring in 5 out of every 10 collisions.

The reaction of $(CF_3)_2C{=}O$ with $(CH_3O)_2PO^-$ was the only reaction where any secondary ion product formation was observed. Scheme II illustrates a suggested reaction pathway which explains formation of the unusual observed primary reaction products. Initial attack by the phosphoryl anion on the carbonyl center results in formation of the adduct at m/z 275. The amount of adduct seen appeared to be dependent on the amount of m/z 219 present in the flow tube. This indicated that only the adduct, m/z 275, was formed by the bimolecular reaction of the cluster ion, $(CH_3O)_2PO^-/H(O{=})P(OCH_3)_2$, with $(CF_3)_2C{=}O$. That adduct formed by reaction of m/z 109 with $(CF_3)_2C{=}O$ apparently contains excess vibrational energy and it is the portion of the adduct that rearranges and fragments into 2. In the adduct, CF_3^- is displaced from the carbon center and then adds to the phosphorus center in 1; this in turn leads to displacement of $^-OCH_3$. The CH_3O^- ion can then react either with 2 producing m/z 147 or it can add to the carbonyl center of neutral $(CF_3)_2C{=}O$ resulting in m/z 197. The product ion m/z 147 can futher react with neutral $(CF_3)_2C{=}O$ by a similar sequence to form adduct m/z 313 and $(CF_3)_2PO^-$ (m/z 185).

The reaction of $(CH_3O)_2PO^-$ with $CH_3C(=O)CH_3$ (reaction 23, Table I) resulted exclusively in total adduct formation (eq 49). The adduct does not further react perhaps due to the fact that there are no good leaving groups available to result in rearrangement.

Scheme II.

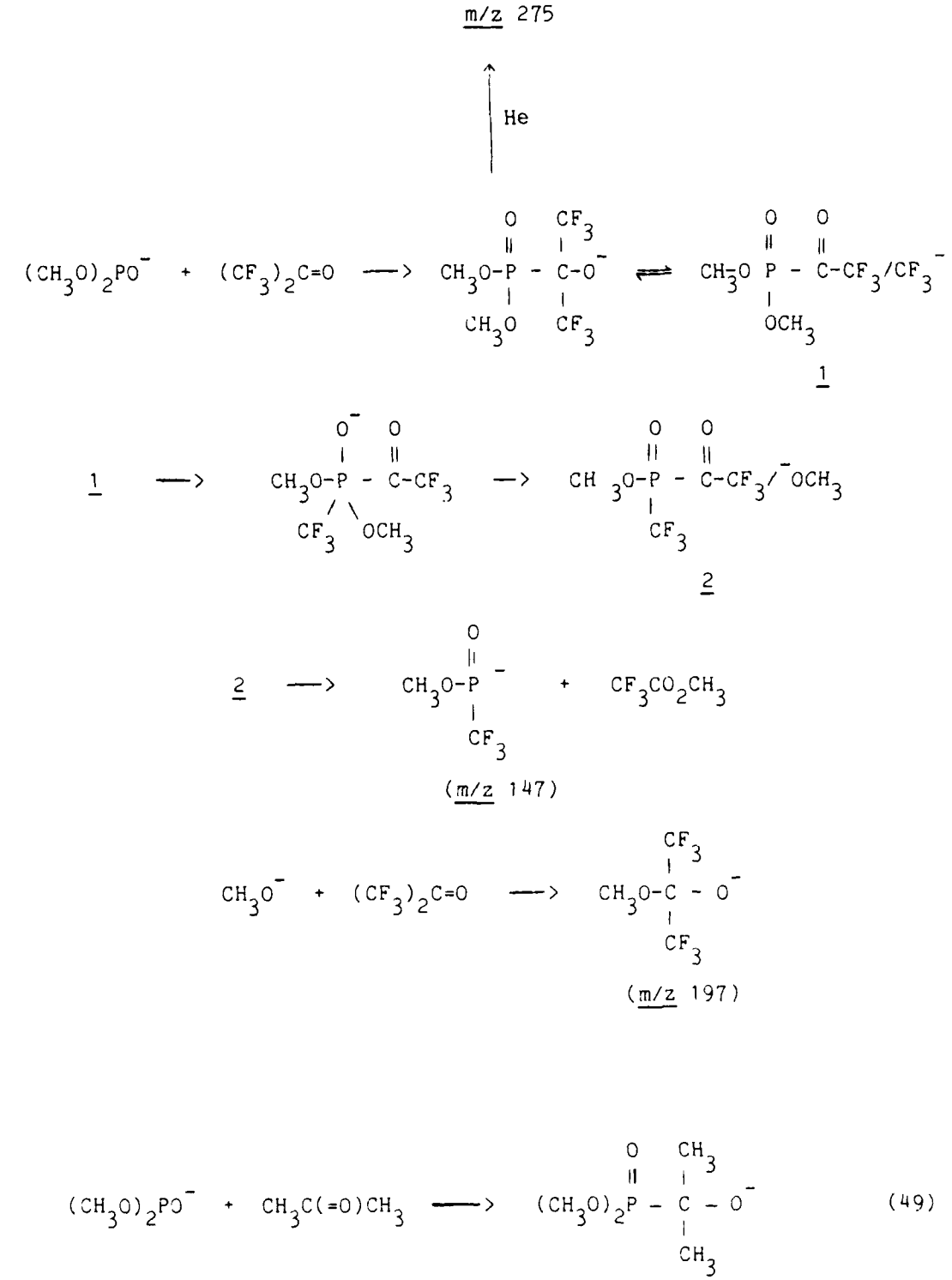
m/z 275
He
(CH3O)2PO⁻ + (CF3)2C=O
1
2
(m/z 147)
CH3O⁻ + (CF3)2C=O
(m/z 197)
(CH3O)2PO⁻ + CH3C(=O)CH3
(49)

H. Reactions of $(CH_3O)_2PO^-$ with Esters.

The reactions of $(CH_3O)_2PO^-$ with the esters $CF_3CO_2CH_3$ (reaction 25, Table I) and $CF_3CO_2C_2H_5$ (reaction 26, Table I) were examined. In both cases (eq 50 and 51), the reactions were slower than that observed with CH_3I and produced $CF_3CO_2^-$ as the major product of S_N2 displacement. The rate of S_N2 displacement follows the gas-phase acidities of HI (ΔH^o_{acid} = 314.6 kcal/mol) and CF_3CO_2H (ΔH^o_{acid} = 323 kcal/mol) as a model for the anions leaving group ability. Minor formation of the total adducts was also observed. The structure of these adducts is suggested to involve nucleophilic addition of phosphoryl anion phosphorus to the carbonyl group of the ester.

$$(CH_3O)PO^- + CF_3CO_2CH_3 \begin{cases} \xrightarrow{0.91} CF_3CO_2^- + (CH_3O)_2P(=O)CH_3 \\ \xrightarrow[He]{0.09} (CH_3O)_2P(=O)C(CF_3)(OCH_3)O^- \end{cases} \quad (50)$$

$$(CH_3O)_2PO^- + CF_3CO_2C_2H_5 \begin{cases} \xrightarrow{0.88} CF_3CO_2^- + (CH_3O)_2P(=O)C_2H_5) \\ \xrightarrow[He]{0.12} (CH_3O)_2P(=O)C(CF_3)(OC_2H_5)O^- \end{cases} \quad (51)$$

I. Reaction of $(CH_3O)_2PO^-$ with Substituted Trifluormethyl Benzenes.

$(CH_3O)_2PO^-$ was allowed to react with $\underline{o}$-$ClC_6H_4CF_3$ (reaction 29, Table I), $\underline{p}$-$BrC_6H_4CF_3$ (reaction 30, Table I), $\underline{m}$-$BrC_6H_4CF_3$ (reaction 31, Table I), and $\underline{o}$-$BrC_6H_4CF_3$ (reaction 32, Table I) to see if a reaction would occur in the gas phase. All four aromatic derivatives react with $(CH_3O)_2PO^-$ in the dark in the condensed-phase giving the products of the $S_{RN}1$ mechanism. The ortho chloro and bromo derivatives did react to form total adducts of unknown structure. The meta and para bromo derivatives did not react.

J. Reactions of the Hydrogen-Bonded Adduct Anion $(CH_3O)_2PO^-/HOP(OCH_3)_2$.

In addition to $(CH_3O)_2PO^-$, its hydrogen bonded adduct $(CH_3O)_2PO^-/HOP(OCH_3)_2$, m/z 219, was also present in the flow under the conditions used in this study. The reactions of the hydrogen bonded adduct with various neutrals and the corresponding reaction rates are summarized in Table V. The products arising from the reaction of m/z 219 with the neutrals used in this study appear to be the same as for $(CH_3O)_2PO^-$. The rates of reaction for the adduct were in most cases slightly faster with higher reaction efficiences compared to those of the phosphoryl anion. This is unusual in many of the reactions studied, especially those of S_N2 displacement. Bohme and his group at York University have shown that coordination of a nucleophile with a hydrogen-bonding molecule slows the rates of S_N2 substitution.[67]

Formation of $(CH_3O)_2PO^-/H(O=)P(OCH_3)_2$ *occurs throughout the length* of the flow tube. A likely reason for the present observed fast rates is that $(CH_3O)_2PO^-/H(O=)P(OCH_3)_2$ is removed both by its reaction with the neutral and by loss of $(CH_3O)_2PO^-$ in its own ion-neutral reaction which makes less of it available to form the hydrogen bonded adduct. Stated simply, the ion intensities of $(CH_3O)_2PO^-$ and $(CH_3O)_2PO^-/H(O=)P(OCH_3)_2$ measured at the end of the flow tube are not those of these ions in the ion-molecule reaction region. The absolute rate constants of the reaction of $(CH_3O)_2PO^-$ are as reported, but those of the cluster $(CH_3O)_2PO^-/H(O=)P(OCH_3)_2$ are only upper limits. The product channel branching fractions may be in error since these values may be composed of product ions formed from both reactant ions.

TABLE VII. Summary of Kinetic and Product Data for the Ion-molecule Reactions of $(CH_3O)_2PO^-/HOP(OCH_3)_2$ with Neutral Molecules.

RXN NO.	NEUTRAL REACTANT	PRODUCT ION + [ASSUMED NEUTRAL]	FRACTION OF PRODUCT	k_{total} $cm^3 molecule^{-1} s^{-1}$	k_{ADO}	EFFICIENCY OF REACTION
1	CH_3Cl -->	No Reaction		$<10^{-13}$		
2a	CH_3Br -->	Br^- + $[(CH_3O)_2P(=O)CH_3]$	0.33	1.2×10^{-12}	1.1×10^{-9}	1.1×10^{-3}
2b	-->	$(CH_3O)_2P(=O)H/Br^-$	0.67			
3	CH_3I -->	I^- + $[(CH_3O)_2P(=O)CH_3]$	1.00	3.4×10^{-11}	9.6×10^{-10}	0.036
4	CF_3Cl -->	No Reaction		$<10^{-13}$		
5a	CF_3Br -->	Br^- + $[(CH_3O)_2PO]$ + $[CF_3]$	0.06	4.0×10^{-10}	4.9×10^{-10}	0.82
5b	-->	$(CH_3O)P(Br)O_2^-$ + $[CF_3CH_3]$	0.94			
6a	CF_3I -->	I^- + $[(CH_3O)_2PO]$ + $[CF_3]$	0.15	6.7×10^{-10}	7.8×10^{-10}	0.86
6b	-->	$(CH_3O)P(I)O_2^-$ + $[CF_3CH_3]$	0.85			

TABLE VII. Summary of Kinetic and Product Data for the Ion-molecule Reactions of $(CH_3O)_2PO^-HOP(OCH_3)_2$ with Neutral Molecules (cont).

7a	$CBrCl_3$	--> CCl_3^- + $[(CH_3O)_2P(O)Br]$	0.22	3.5×10^{-10}	7.8×10^{-10}	0.44
7b		--> $(CH_3O)P(Br)O_2^-$ + $[CCl_3CH_3]$	0.54			
7c		--> $CBrCl_2^-$ + $[(CH_3O)_2P(=O)Cl]$	0.24			
8	$CHCl_3$	$\xrightarrow{He}$ $(CH_3O)_2PO^-/HCCl_3$	1.00	5.2×10^{-11}	9.1×10^{-10}	0.038
9a	CCl_4	--> CCl_3^- + $[(CH_3O)_2P(=O)Cl]$	0.81	8.8×10^{-11}	8.0×10^{-10}	0.11
9b		--> $(CH_3O)P(Cl)O_2^-$ + $[CH_3CCl_3]$	0.19			
10a	CCl_3F	--> CCl_2F^- + $[(CH_3O)_2P(=O)Cl]$	0.79	1.9×10^{-11}	8.0×10^{-10}	0 .024
10b		--> $(CH_3O)P(Cl)O_2^-$ + $[CCl_2FCH_3]$	0.17			
10c		--> CCl^- + $[(CH_3O)_2P(=O)CCl_2F]$	0.04			
11a	CCl_2F_2	--> $(CH_3O)P(O)_2Cl^-$ + $[CClF_2CH_3]$	0.43	8.7×10^{-13}	8.6×10^{-10}	1.0×10^{-3}
11b		--> $(CH_3O)_2P(=O)H/Cl^-$ + $[(CH_3O)_2P(=O)CClF_2]$	0.57			

TABLE VII. Summary of Kinetic and Product Data for the Ion-molecule Reactions of $(CH_3O)_2PO^-HOP(OCH_3)_2$ with Neutral Molecules (cont).

12a	CCl_2FCClF_2 -->	$(CH_3O)P(O)_2Cl^-$ + $[CCl_2FCF_2CH_3]$	0.14	2.7×10^{-10}	5.0×10^{-10}	0.53
12b	-->	$(CH_3O)_2P(=O)H/Cl^-$ + $[(CH_3O]_2P(O)CF_2CCl_2F]$	0.86			
13	$CHClF_2$ $\xrightarrow{He}$	$(CH_3O)_2PO^-/HCClF_2$	1.00	6.1×10^{-12} a	8.0×10^{-10}	7.6×10^{-3}
14	CH_2Cl_2 $\xrightarrow{He}$	$(CH_3O)_2PO^-/H_2CCl_2$	1.00	2.6×10^{-12} a	1.2×10^{-9}	2.2×10^{-3}
15	CO_2 $\xrightarrow{He}$	$(CH_3O)_2POCO_2^-$	1.00	1.0×10^{-13} a	6.1×10^{-10}	1.64×10^{-4}
16	SO_2 $\xrightarrow{He}$	$(CH_3O)_2POSO_2^-$	1.00	4.5×10^{-10} a	1.2×10^{-9}	0.38
17a	H_2S -->	$(CH_3O)_2P(=O)H$ / ^-SH	0.67	2.6×10^{-10}	1.2×10^{-9}	0.22
17b	-->	$(CH_3O)P(O)_2H^-$ + $[CH_3SH]$	0.23			
17c	-->	$(CH_3O)_2P(=O)H/(O)_2(H)P(OCH_3)^-$	0.10			

TABLE VII. Summary of Kinetic and Product Data for the Ion-molecule Reactions of $(CH_3O)_2PO^-HOP(OCH_3)_2$ with Neutral Molecules (cont).

18a	CH_3SH --> $(CH_3O)P(H)O_2^-$ + $[CH_3SCH_3]$	0.61	8.6×10^{-13}	1.2×10^{-9}	7.2×10^{-4}
18b	--> $(CH_3O)_2P(H)O_2^-/H(O=)P(OCH_3)_2$	0.39			
19a	C_2H_5SH --> $C_2H_5S^-$ + $[(CH_3O)_2P(=O)H]$	0.04	1.7×10^{-12}	1.2×10^{-9}	1.4×10^{-3}
19b	--> $C_2H_5SH/SC_2H_5^-$	0.10			
19c	--> $(CH_3O)P(H)O_2^-$ + $[C_2H_5SCH_3]$	0.48			
19d	--> $(CH_3O)_2PO/HSC_2H_5^-$	0.10			
19e	--> $(CH_3O)_2P(H)O_2^-/H(O=)P(OCH_3)_2$	0.28			
21	CH_3NO_2 --> $(CH_3O)_2PO/CH_3NO_2^-$	1.00	8.5×10^{-12}	1.9×10^{-9}	4.5×10^{-3}
22	CF_3CH_2OH --> $(CH_3O)_2PO^-/HOCH_2CF_3$	1.00	Not measured		

TABLE VII. Summary of Kinetic and Product Data for the Ion-molecule Reactions of $(CH_3O)_2PO^-HOP(OCH_3)_2$ with Neutral Molecules (cont).

23a	$(CF_3)_2C=O$ -->	$(CH_3O)_2P(=O)C(CF_3)_2O^-$	0.17	6.0×10^{-10}	9.2×10^{-10}	0.66
23b	-->	$CH_3OP(O)(CF_3)^-$ + $[CH_3C(O)CF_3]$	0.50			
23c	-->	$CH_3OC(O)(CF_3)_2^-$ + $[(CH_3O)P(=O)]$	0.33			
23d	-->	$(CF_3)_2PO^-$ (secondary product)				
23e	-->	$(CH_3O)(CF_3)P(O)/C(O)(CF_3)_2^-$ (secondary product)				
24	$(CH_3)_2C=O$ -->	$(CH_3O)_2P(=O)C(CH_3)_2O^-$	1.00	5.8×10^{-13} [b]	1.5×10^{-9}	3.9×10^{-4}
25a	$CF_3CO_2CH_3$ $\xrightarrow{He}$	$(CH_3O)_2P(=O)/CF_3CO_2CH_3^-$	0.09	7.7×10^{-12} [a]	1.3×10^{-9}	5.9×10^{-3}
25b	-->	CF_3CO^- + $[(CH_3O)_2P(=O)CF_3]$	0.91			
26a	$CF_3CO_2C_2H_5$ $\xrightarrow{He}$	$(CH_3O)_2P(=O)/CF_3C(O)C_2H_5^-$	0.12	7.6×10^{-12} [a]	1.3×10^{-9}	5.8×10^{-3}
26b	-->	CF_3CO^- + $[(CH_3O)_2P(=O)C_2H_5]$	0.88			

[a] Apparent bimolecular rate constant for termolecular process. [b] Kinetic data at 1.00 torr only.

V. CONCLUSIONS

The dimethoxy phosphoryl anion, $(CH_3O)_2PO^-$, is readily prepared in the gas-phase through ion-molecule reaction with phenyl nitrene anion radical (PhN^-). The hydrogen bonded adduct of dimethyl phosphite and dimethoxy phosphoryl anion, $(CH_3O)_2PO^-/H(O=)P(OCH_3)_2$, can also be produced and studied under the same conditions.

$(CH_3O)_2PO^-$ is an ambident species of low acidity and intrinsic nucleophilicity. It reacts with polyhalogenated alkanes through an electron transfer process similiar to the initial step in the $S_{RN}1$ mechanism. The dimethoxy phosphoryl anion adds to carbonyl or sulfonyl centers to form stable adduct anions. Hydrogen bonding of $(CH_3O)_2PO^-$ to protic species appears to be the preferred reaction pathway in the gas-phase for this anion.

APPENDIX I.

Diffusion of negative ions to the walls of the flow tube in the flowing afterglow apparatus (FA) is a possible source of error in determining absolute rates and branching fraction for ion-molecule reactions. In order to determine the significance, if any, of diffusion in this study, it is necessary to set up and evalutate the rate equations associated with the ion-molecule reactions studied in the FA. To accomplish this evaluation and to determine the integrity of the flowing afterglow/mass spectrometer in the measurement of the ion product branching fractions, a model using diffusion and a model without diffusion will be evaluated and compared to actual results. A determinination of the significance of diffusion will be extrapolated from this comparison.

A. Kinetic Model without Diffusion.

The model to be used for this derivation will consider only the bimolecular rate equations for the formation of product ions from a starting ion and an added neutral substrate. Consideration was given in earlier studies[50] to quenching of species in the flow tube by the carrier gas and the possibility of quenching of the metastables in the flow tube by the neutral substrate being added to the flow. In order to insure in this study that all the metastables formed were quenched prior to the introduction of the neutral reactant, a small amount of nitrogen or argon gas was also introduced into the flow to quench any metastables that might have been produced in the electron gun region. The addition of SF_6 down stream in the flow tube was an additional check to insure that all quenching had occured prior to the ion-molecule neutral inlet.

In all cases, no electrons were detected downstream in the flow tube and therefore all metastables were quenched. Eq A.1 and A.2 are the rate expressions for the formation of products and decay of starting ion signal. Q^- is the starting ion with $k_{tot}[N]$ is the observed psuedo first order rate constant for decay. P_i^- are the individual product

$$-d[Q^-]/dt = k_{total}[N][Q_o^-] \quad (A.1)$$

$$d[P_i^-]/dt = k_i[N][Q^-] \quad (A.2)$$

ions and $k_i[N]$ are the individual pseudo first order rate constants for product formation as derived from branching fractions obtained from mass spectral data. The integrated form of the rate equations become (eq A.3 and A.4):

$$[Q^-] = [Q_o^-]\exp-(k_{total}[N])t \quad (A.3)$$

$$[P_i^-] = \frac{-k_i[Q_o^-]\{\exp-(k_{total}[N]t) - 1\}}{k_{total}} \quad (A.4)$$

B. Kinetic Model with Diffusion.

A different set of rate equations is obtained when diffusion is included as a loss process for ions in the flow tube. These processes are shown in eq A.5 and A.6.

$$Q^- \xrightarrow{k_w} \text{wall} \quad (A.5)$$

$$P_i^- \xrightarrow{k_{wi}} \text{wall} \quad (A.6)$$

The differential rate equations are now given by eq A.7 and A.8.

$$-d[Q^-]/dt = k_{total}[Q_o^-][N] + k_w[Q^-] \quad (A.7)$$

$$d[P_i^-]/dt = k_i[Q^-][N] - k_{wi}[P_i^-] \quad (A.8)$$

The rate constants k_w and k_{wi} represent the rate constants for diffusion to the wall of the flow tube.

The rate constant for diffusion (k_w or k_{wi}) can be defined (eq A.9) in terms of the pressure independent diffusion coefficient, D_o, where

$$k_w = D_o/\Lambda^2[M]n \qquad (A.9)$$

[M] is the concentration of the carrier gas (3.26×10^{16} molecules cm^{-3} at a pressure of 1.0 torr), n is the correction factor for parabolic flow (1.59),[44] and Λ is the diffusion length as defined in eq A.10.

$$\Lambda^{-2} = (\pi/L)^2 + (4.82/d)^2 \qquad (A.10)$$

L is the length and d is the diameter of the flow tube.[36,51] For the tube used in these experiments, d is 7.15 cm and L is 66 cm when the substrate gas is introduced at the ion-molecule neutral inlet in Figure 1. The value for Λ^{-2} is then 0.4567 cm^{-2}. Time is held constant in this study and can be claculated using eq A.11.

$$t = \frac{L}{\bar{v}} \qquad (A.11)$$

It can be shown[51] that eq A.5 and A.6, when evaluated, yield integrated rate equiations A.12 and A.13.

$$[Q^-] = [Q_o^-] \exp-(k_w + k_{total}[N])t \qquad (A.12)$$

$$[P_i^-] = \frac{k_i[Q_o^-][N] \quad [\exp(-k_w - k_{total}[N])t - \exp(-k_{wi}t)]}{(k_{wi} - k_w - k_{total}[N])} \qquad (A.13)$$

The rate constants for diffusion, k_w and k_{wi}, are proportional to D_o, the diffusion coefficient (eq A.9). The diffusion coefficients for the species in this study are not all known, however, D_o has been shown to be inversely proportional to the square root of the reduced mass, μ, of the ions considered.[52]

C. Comparison of Experimental and Calculated Data.

In order to determine the effect that diffusion has on the results of this study, the reaction of $(CH_3O)_2PO^-$ with CCl_2FCClF_2 (Table I, reaction) was modeled using rate equations with diffusion and rate equations without diffusion. The results are compared to the experimental values obtained. The experimental data is listed in Table A.I and the data is plotted in Figure A.1. For the purpose of this comparison, the cluster product, m/z 145 will be treated as Cl^- (eq A.14). All peak areas were normalized to $[m/z\ 109]_o = 1.00$. The experiment was conducted with $P_{He} = 0.5$ torr, $\bar{v} = 82.3$ m/s, and t = 0.0079 s. The experimentally observed rate constant was 2.6×10^{-10} cm^3/molecule-s.

$$\begin{array}{l} \xrightarrow{0.86} \underset{m/z\ 35}{Cl^-} + (CH_3O)_2P(=O)CClFCClF_2 \\ (CH_3O)_2PO^- + CCl_2FCClF_2 \xrightarrow{0.01} \\ m/z\ 109 \\ \xrightarrow{0.14} \underset{m/z\ 129}{(CH_3O)P(Cl)O_2^-} + CClF_2CClFCH_3 \end{array} \qquad (A.14)$$

The same reaction (eq A.14) was used for the calculation using the *model without diffusion*. The decay of the starting ion and the formation of products were calculated using equations A.3 and A.4, respectively. The calculated data is listed in Table A.II and is plotted in Figure A.2.

Finally, the model using diffusion (eq A.12 and A.13) was used to calculated values for the decay of starting ion and formation of products ions for the reaction of $(CH_3O)_2PO^-$ with CCl_2FCClF_2. Calculated data is listed in Table A.III and plotted in Figure A.3.

TABLE A.I. Experimental Data for the Reaction of $(CH_3O)_2PO^-$ with CCl_2FCClF_2

CCl_2FCClF_2 (molecules/cm^3)	INTEGRATED AREA OF MASS SPECTRA PEAKS		
	m/z 109	m/z 35	m/z 129
0	1.00	0	0
2.73×10^{11}	0.787	0.143	0.025
4.09×10^{11}	0.707	0.249	0.044
5.36×10^{11}	0.507	0.386	0.070
6.89×10^{11}	0.226	0.551	0.096
1.04×10^{12}	0.198	0.639	0.102
1.41×10^{12}	0.079	0.786	0.116

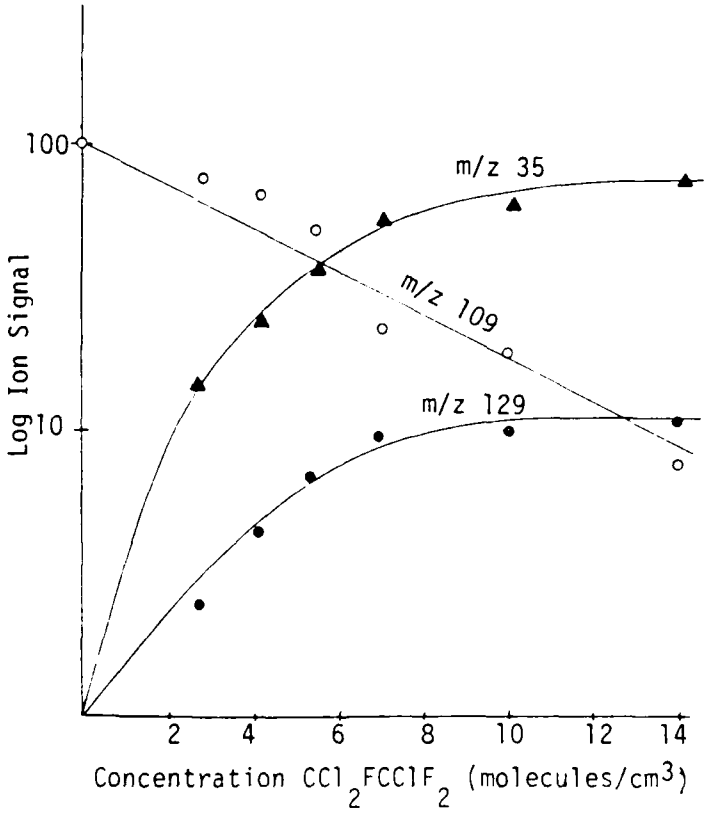

Figure A.1. Semilogrithmic plot of experimental data for decay of m/z 109 and formation of m/z 35, m/z 129, and m/z 145.

TABLE A.II. Calculated Data for the Reaction of $(CH_3O)_2PO^-$ with CCl_2FCClF_2 Using Model Without Diffusion.

CCl_2FCClF_2 (molecules/cm^3)	CALCULATED AREA OF MASS SPECTRA PEAKS		
	m/z 109	m/z 35	m/z 129
0	1.00	0	0
2.73×10^{11}	0.703	0.255	0.042
4.09×10^{11}	0.590	0.353	0.057
5.36×10^{11}	0.500	0.430	0.070
6.89×10^{11}	0.411	0.507	0.082
1.04×10^{12}	0.261	0.636	0.103
1.41×10^{12}	0.162	0.721	0.117

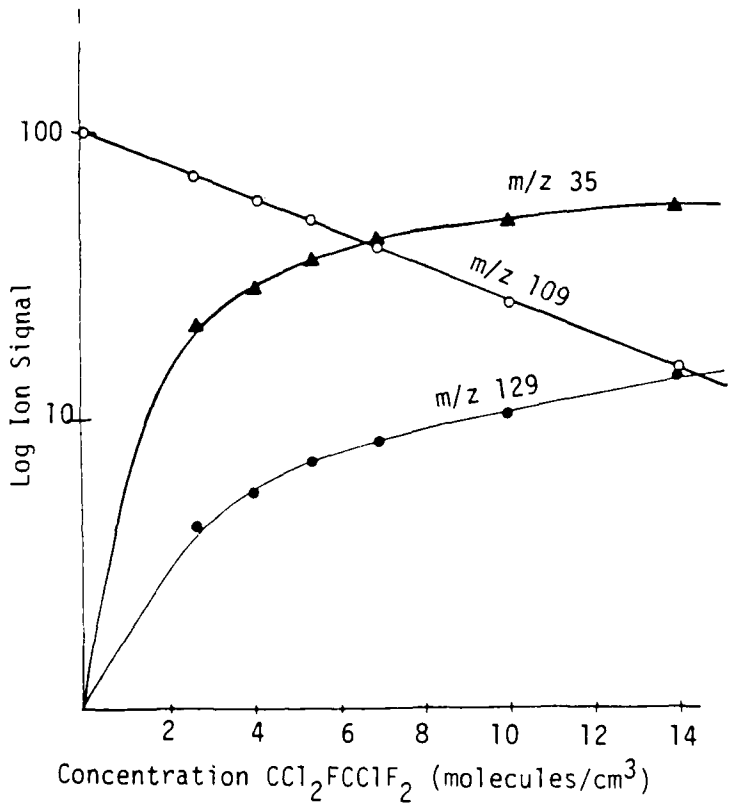

Figure A.2. Semilogrithmic plot of calculated data for decay of m/z 109 and formation of m/z 35, m/z 129, and m/z 145 using model without diffusion.

TABLE A.III. Calculated Data for the Reaction of $(CH_3O)_2PO^-$ with CCl_2FCClF_2 Using Model With Diffusion.

CCl_2FCClF_2 (molecules/cm^3)	CALCULATED AREA OF MASS SPECTRA PEAKS m/z 109	m/z 35	m/z 129
0	1.00	0	0
2.73×10^{11}	0.702	0.227	0.043
4.09×10^{11}	0.589	0.303	0.059
5.36×10^{11}	0.501	0.364	0.070
6.89×10^{11}	0.411	0.426	0.084
1.04×10^{12}	0.260	0.530	0.106
1.41×10^{12}	0.162	0.592	0.158

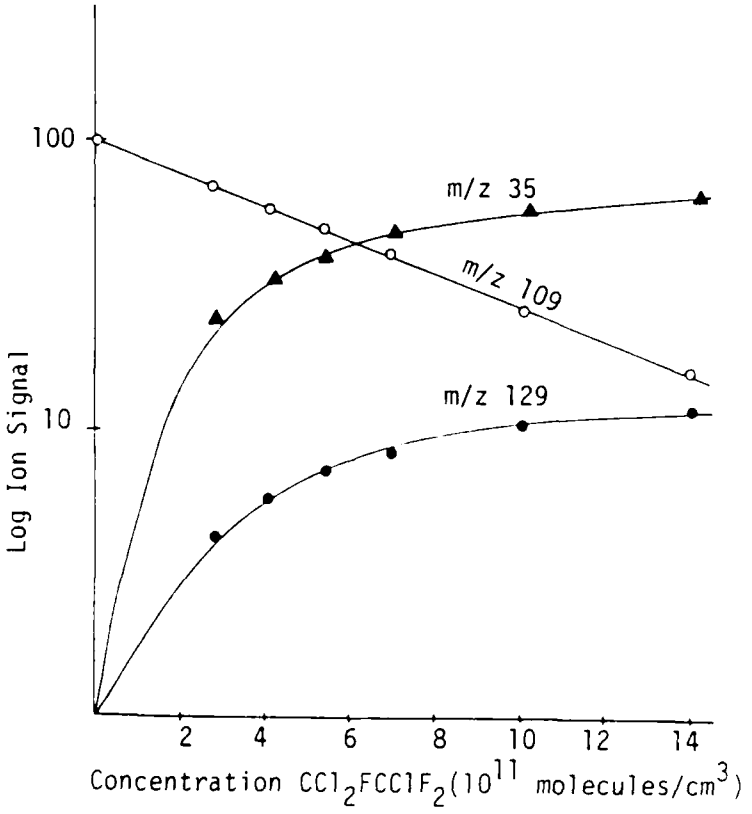

Figure A.3. Semilogrithmic plot of calculated data for decay of m/z 109 and the formation of m/z 35, m/z 129, and m/z 145 using model with diffusion.

TABLE A.IV. Diffusion Coefficients in Helium and Diffusion Rate Constants.

ION	D_o (10^{19} cm^{-1} s^{-1})	k_w[a] (s^{-1})
m/z 109	0.963[b]	135
m/z 35	1.41[c]	197
m/z 129	0.938[d]	131

[a]Parabolic flow factor omitted. [b]Extrapolated from values in ref 56. [c]Ref 56. [d]Assigned D_o for SF_5^- (m/z 127), ref 56.

Table A.IV lists the diffusion coefficients used in the calculation. D_os for all the ions in this study are not available. D_o for similiar molecular weight ions were used or values extrapolated from given values.[56] Table A IV lists the diffusion coefficient data that was used to calculate k_w and k_{wi} for this reaction.

D. Conclusions.

It is evident from the above comparison that diffusion must be considered in the flowing afterglow apparatus. There is a large loss of ions to diffusion in such a system. It also effects the branching fractions of the product ions. This affect is significant if the difference in mass of the product ions is large or the products ions are of relatively small mass compared to the starting ion. Small mass ions are lost to the walls of the flow tube at a much faster rate than the larger mass ions. The observed total rate constant, however, is not effected by the diffusion phenomena. The reactions of $(CH_3O)_2PO^-$ yield greatly varying mass ions as products and therefore the branching

fractions are only indicatiors as to the relative ratios of products for a given reaction in the gas-phase. When reactions involve similiar mass product ions, the branching fractions are reasonably accurate, especially when other mass descrimination factors are taken into account.

REFERENCES

(1) Corbridge, D. E. C. "Phosphorus: An Outline of its Chemistry, Biochemistry and Technology", Elsevier Scientific Publishing Company, New York, 1978.

(2) Kirby, A. J.; Warren, S. G.; "The Organic Chemistry of Phosphorus", Elsevier Publishing Co., New York, 1967, Chap. 2,3,4, and 7.

(3) Emsley, J.; Hall, D. "The Chemistry of Phosphorus", Halsted Press, New York, 1976, Chap. 8 and 12.

(4) Hodges, R. V.; McDonnell, T. J.; Beauchamp, J. L. J. Am. Chem. Soc., 1980, 102, 1327-1332.

(5) Anderson, D. R.; DePuy, C. H.; Filey, J.; Bierbaum, V. M. J. Am. Chem. Soc., 1984, 106, 6513-6517.

(6) Hodges, R. V.; Houle, F. A.; Beauchamp, J. L.; Montag, R. A.; Verkade, J. G. J. Am. Chem. Soc., 1980, 102, 932-935.

(7) Holtz, D.; Beauchamp, J. L.; Eyler, J. R. J. Am. Chem. Soc., 1970, 92, 7045-7055.

(8) Holtz, D.; Beauchamp, J. L. J. Am. Chem. Soc., 1969, 91, 5913-5915.

(9) Staley, R. H.; Beauchamp, J. L. J. Am. Chem. Soc., 1974, 96, 6252-6259.

(10) MacNeil, K. A. G.; Thynne, J. C. J. J. Phys. Chem., 1970, 74, 2257-2262.

(11) Sullivan, S. A.; Beauchamp, J. L. Inorganic Chemistry, 1978, 17, 1589-1595.

(12) Asubiojo, O. I.; Brauman, J. I. J. Am. Chem. Soc., 1977, 99, 7707-7708.

(13) Pietro, W. J.; Hehre, W. J. J. Am. Chem. Soc., 1982, 104, 3594-3595.

(14) Kenttamaa, H. I.; Cooks, R. G. J. Am. Chem. Soc., 1985, 107, 1881-1886.

(15) Zwinselman, J. J.; Ciommer, B.; Schwarz, H. In "Tandem Mass Spectrometry," McLafferty, F. W., Ed.; Wiley; New York, 1983, Chapter .

(16) Diekman, J.; MacLeod, J.; Djerassi, C.; Baldeschwieler, J. D. J. Am. Chem. Soc., 1969, 91, 2069-2084.

(17) Holmes, J. L.; Lossing, F. P. J. Am. Chem. Soc., 1980, 102, 1591-1595.

(18) Lewis, E. S.; Spears, L. G. J. Am. Chem. Soc., 1985, 107, 3918-3921.

(19) Clapp, C. H.; Westheimer, F. H., J. Am. Chem. Soc., 1974, 96, 6710-6714.

(20) Satterthwait, A. C.; Westheimer, F. H. J. Am. Chem. Soc., 1980, 102, 4464-4472.

(21) Satterthwait, A. C.; Westheimer, F. H. J. Am. Chem. Soc., 1981, 103, 1177-1180.

(22) Ramirez, F.; Marecek, J. F. J. Am. Chem. Soc., 1979, 101, 1460-1465.

(23) Ramirez, F.; Marecek, J. F. J. Am. Chem. Soc., 1982, 104, 1345-1349.

(24) Kornblum, N.; Boyd, S. D. J. Am. Chem. Soc., 1970, 92, 5748-5758.

(25) Meyerson, S.; Harvan, D. J.; Hass, J. R.; Rameriz, F.; Mareck, J. F. J. Am. Chem. Soc., 1984, 106, 6877-6883.

(26) Rameriz, F.; Marecek, J.; Minore, J.; Srivastava, S.; le Noble, W. J. Am. Chem. Soc., 1986, 108, 348-349.

(27) Henchman, M.; Viggiano, A. A.; Paulson, J. F. J. Am. Chem. Soc., 1985, 107, 1453-1455.

(28) Jamdagni, R.; Kebarle, P. J. Am. Chem. Soc., 1971, 93, 7139-7143.

(29) Bunnett, J. F. Acc. Chem. Res., 1978, 11, 413-420.

(30) a) Kornblum, N.; Michel, R. E.; Kerber, R. C. J. Am. Chem. Soc., 1966, 88, 5663. b) Kornblum, N. Angew. Chem. Int. Ed. Engl., 1975, 14, 734-745.

(31) a) Russell, G. A.; Danen, W. C. J. Am. Chem. Soc., 1966, 88, 5663. b) Russell, G. A.; Danen, W. C. J. Am. Chem. Soc., 1968, 90, 347.

(32) Amatore, C.; Combellas, C.; Pinson, J.; Oturan, M. A.; Robveille, S.; Saveant, J.; Thiebault, A. J. Am. Chem. Soc., 1985, 107, 4846-4853.

(33) Rossi, R. A.; de Rossi, R. H. "Aromatic Nucleophilic Substitution by the $S_{RN}1$ Mechanism", American Chemical Society, Washington DC, 1983, ACS Monogr. No. 78.

(34) Amatore, C.; Oturan, M. A.; Pinson, J.; Saveant, J.; Thiebault, A. J. Am. Chem. Soc., 1985, 107, 3451-3459.

(35) Bunnett, J. F.; Creary, X. J. Org. Chem., 1974, 39, 3612-3614.

(36) Bunnett, J. F.; Hoz, S. J. Am. Chem. Soc., 1977, 99, 4690-4699.

(37) Bunnett, J. F.; Creary, X. J. Org. Chem., 1974, 39, 3611-3612.

(38) Bunnett, J. F.; Traber, R. P. J. Org. Chem., 1978, 43, 1867-1872.

(39) Ferguson, E. E.; Fehsenfeld, F. C.; Schmeltekopf, A. L. Adv. At. Mol. Phys., 1969, 5.

(40) McDonald, R. N.; Chowdhury, A. K.; Setser, D. W. J. Am. Chem. Soc. 1980, 102, 6491-6498.

(41) McDonald, R. N.; Chowdhury, A. K. J. Am. Chem. Soc., 1985, 107, 4123-4128.

(42) Huggins, R. W.; Cahn, J. H. J. Appl. Phys., 1967, 38, 180.

(43) Drazaic, P. S.; Marks, J.; Brauman, J. I. In "Gas Phase Ion Chemistry," Bowers, M.T., Ed.; Acedemic Press: New York, 1984; Vol. 3, Chapter .

(44) Stafford, G. C. "Instrumental Aspects of Positive and Negative Ion Chemical Ionization Mass Spectrometry," presented to the American Society for Mass Spectrometry, Seattle, Washington, June, 1979.

(45) Su, T.; Bowers, M. T. J. Chem. Phys., 1973, 58, 3027.

(46) Su. T.; Bowers, M. T. J. Am. Chem. Soc., 1973, 95, 1370.

(47) Miller, K. J.; Savchik, J. A. J. Am. Chem. Soc., 1979, 101, 7206-7213.

(48) Su, T.; Bowers, M. T. Int. J. Mass Spectrom. Ion Phys., 1973, 12, 347-356.

(49) Benson, S. W. "Thermochemical Kinetics," 2nd ed,; Wiley; New York, 1976.

(50) Jones, M. T., Masters Thesis, Kansas State University, 1983.

(51) Kolts, J. M.; Setser, D. W. "Reactive Intermediates In the Gas Phase," Setser, D. W., Ed.; Academic Press, New York: 1979, Chapter 3.

(52) Hirschfelder, J. O.; Curtiss, C. F.; Bird, R. B. "Molecular Theory of Gases and Liguids," Wiley, New York, 1965.

(53) Christodoulides, A. A.; McCorkle, D. L.; Christophorou, L. G. In "Electron Molecule Interactions," Christodoulides, A. A., Ed.; Academic Press: New York, 1984, Chapter 6.

(54) Bartess, J. E.; McIver, R. T. In "Gas Phase Ion Chemistry," Bowers, M. T., Ed.; Academic Press: New York, 1979, Chapter 11.

(55) Dotan, I.; Lindinger, W.; Albritton, D. L. J. Chem. Phys., 1976, 64, 4544.

(56) Based on $\Delta H_f^o(F_3CI)$ = -140.6 kcal,[57] $EA(F_3CI)$ = -36.8 kcal,[53] $\Delta H_f^o(I^-)$ = -44.9 kcal,[58] $\Delta H_f^o(\cdot CF_3)$ = -111.1 kcal,[49] $D^o(F_3C-I^-)$ = 21.4 kcal.

(57) Cox, J. D.; Pilcher, G. "Thermochemistry of Organic and Organometallic Compounds," Academic Press: New York, 1970.

(58) Rosenstock, H. M.; Draxl, K.; Steiner, B. W.; Herron, J. T. "Journal of Physical and Chemical Data," American Chemical Society and American Institute of Physics, 1977, Vol.6, Supplement 1.

(59) McMillen, D. F.; Golden, D. M. Amm. Rev. Phys. Chem., 1982, 33, 493-532.

(60) Based on $\Delta H_f^o(CCl_4)$ = -26.3 $\pm$ 0.6 kcal,[57] $\Delta H_f^o(Cl)$ = 28.9 kcal,[49] $\Delta H_f^o(\cdot CCl_3)$ = 18.5 kcal.[49]

(61) Based on $\Delta H_f^o(CCl_3F)$ = -64 $\pm$ 2 kcal,[57] $\Delta H_f^o(Cl)$ = 28.9 kcal.[49]

(62) Based on $\Delta H_f^o(CBrCl_3)$ = -9.3 $\pm$ 2.0 kcal,[57] $\Delta H_f^o(Br)$ = 26.7 kcal,[49] $\Delta H_f^o(\cdot CCl_3)$ = 18.5 kcal.[49]

(63) Based on $\Delta H_f^o(CF_3Cl)$ = -169.4 $\pm$ 0.7 kcal,[57] $\Delta H_f^o(Cl)$ = 28.9 kcal,[49] $\Delta H_f^o(\cdot CF_3)$ = -111.1 kcal.[49]

(64) Based on $\Delta H_f^o(CF_3Br)$ = -154 kcal,[57] $\Delta H_f^o(Br)$ = 26.7 kcal,[49] $\Delta H_f^o(^{\cdot}CF_3)$ = -111.1 kcal.[49]

(65) Smith, D.; Adams, N. G.; Alge, E. J. Phys. B: At. Mol. Phys., 1984, 17, 461-472.

(66) Popkie, H. E.; Kaufman, J. J. Chem. Phys. Lett., 1977, 47, 55.

(67) a) Bohme, D. K.; Raksit, A. B. J. Am. Chem. Soc., 1984, 106, 3447-3452. b) Bohme, D. K.; Mackay, G. I. J. Am. Chem. Soc., 1981, 103, 978.

ACKNOWLEDMENTS

I would first like to offer my appreciation to my research advisor, Dr. Richard N. McDonald for his guidance and encouragement of this research. I would also like to thank my laboratory colleges, Phillip Schell, Micheal Jones, and A. K. Chowdury for tireless patience in their instruction on tne flowing afterglow apparatus and on their insights and enlightenments as I stumbled through interpreting results of this study.

Appreciation is expressed the U.S. Army Research Office and the National Science Foundation for the support of this research and to the United Stated Army and Chemical Corps for affording me this opportunity to further my education.

Most of all I thank my husband, Lloyd, for his continued support,unwavering confidence, and supreme sacrifices which have allowed me to pursue my career.

END

DTIC

7-86